JOURNAL OF PETROLOGY | VOLUME 36 | NUMBER 5 | PAGES 1393–1432 | 1995

L. MELLUSO[1*], L. BECCALUVA[2], P. BROTZU[1], A. GREGNANIN[3], A. K. GUPTA[4], L. MORBIDELLI[5] AND G. TRAVERSA[5,6]

[1]DIPARTIMENTO DI SCIENZE DELLA TERRA, UNIVERSITÀ DI NAPOLI 'FEDERICO II', VIA MEZZOCANNONE 8, I-80134 NAPOLI, ITALY
[2]ISTITUTO DI MINERALOGIA, UNIVERSITÀ DI FERRARA, ITALY
[3]DIPARTIMENTO DI SCIENZE DELLA TERRA, UNIVERSITÀ DI MILANO, ITALY
[4]DEPARTMENT OF GEOLOGY, ALLAHABAD UNIVERSITY, ALLAHABAD, INDIA
[5]DIPARTIMENTO DI SCIENZE DELLA TERRA, UNIVERSITÀ DI ROMA, ITALY
[6]DIPARTIMENTO DI SCIENZE DELLA TERRA, UNIVERSITÀ DI PERUGIA, ITALY

Constraints on the Mantle Sources of the Deccan Traps from the Petrology and Geochemistry of the Basalts of Gujarat State (Western India)

The late Cretaceous–early Tertiary flood basalts in the Gujarat area of the northwestern Deccan Traps (Kathiawar peninsula, Pavagadh hills and Rajpipla) exhibit a wide range of compositions, from picrite basalts to rhyolites; moreover, the basaltic rocks have clearly distinct TiO_2 contents at any given degree of differentiation and strongly resemble the low-titanium and high-titanium basalts found in most of the Gondwana continental flood basalt (CFB) suites. Four magma groups are petrologically and geochemically distinguished:

(1) A low-Ti group, characterized by rocks with varying SiO_2 saturation, and with TiO_2 <1·8 wt %, extremely low incompatible trace element abundances, low Zr/Y (av. 3·8), Ti/V (av. 27), and a very slight large ion lithophile element (LILE) enrichment over high field strength elements (HFSE). These rocks share some features with the Bushe Formation of the Western Ghats farther south, but have distinct geochemical characters, in particular the strong depletion in most incompatible trace elements.

(2) A high-Ti group, characterized by a more K-rich character than the low-Ti rocks, and with a strong enrichment in incompatible elements, similar to average ocean island basalt (OIB), e.g. high TiO_2 (>1·8 wt % in picrites), Nb (>19 p.p.m.) Zr/Y (av. 6·5) and Ti/V (av. 47).

(3) An intermediate-Ti group, with TiO_2 contents slightly lower than the high-Ti rocks at the same degree of evolution, and with correspondingly lower incompatible trace element contents and ratios, in particular K_2O, Nb, Ba and Zr/Y (av. 5·2).

(4) A potassium-rich group (KT), broadly similar in geochemical character to the high-Ti group but showing more extreme K, Rb and Ba enrichment (av. $K_2O/Na_2O \sim 1$; Ba/Y ~ 20).

The most primitive low-Ti and high-Ti picrites, when corrected for low-pressure olivine fractionation, show distinct major (and trace) element geochemistry, in particular for CaO/Al_2O_3, CaO/TiO_2 and Al_2O_3/TiO_2, and moderate but significant variations in their SiO_2 and Fe_2O_{3t} contents; these characteristics strongly suggest the involvement of different mantle sources, more depleted for the low-Ti picrites, and richer in cpx for the high-Ti picrites, but with broadly the same pressures of equilibration (27–14 kbar). This, in turn, suggests a strong lateral heterogeneity in the Gujarat Trap mantle. Low-Ti picrites and related differentiates in Kathiawar are reported systematically for the first time here, and suggest the existence of HFSE-depleted mantle in the northwestern Deccan Traps, with extension at least to the Seychelles Islands and to the area of the Bushe Formation near Bombay in the pre-drift position, before the development of the Carlsberg Ridge. The absence of correlations between LILE/HFSE ratios and SiO_2 argues against crustal contamination processes acting on the low-Ti picrites, possibly owing to their probably rapid uprise to the surface. Consequently, the mantle region of this rock group was probably re-enriched by small amounts of LILE-rich materials. The substantially higher trace element enrichment of the least differentiated high-Ti picrites, relative to the basalts of the Ambe-

*Corresponding author. e-mail: melluso@ds.cised.unina.it

nali and Mahableshwar Formations of the Western Ghats, testifies also to the presence of more incompatible element rich, OIB-like mantle sources in northern and northwestern Gujarat. These sources were geochemically similar to the present-day Reunion mantle sources.

KEY WORDS: *Deccan Traps; geochemistry; petrology; picrite basalts; western India*

INTRODUCTION

The Deccan Traps of western India are one of the most voluminous Phanerozoic continental flood basalt (CFB) provinces; they cover an area of $\sim 0{\cdot}5 \times 10^6$ km^2 on land, but a significant part of the volcanic sequence lies on the nearby continental shelf, and there are coeval but volumetrically minor volcanic rocks in the Seychelles Islands (see Backman *et al.*, 1988; Devey & Stephens, 1991). The eruption of this large volume of basaltic rocks [$(1–2) \times 10^6$ km^3] took place within a very narrow time span, from the end of Cretaceous to the very early Tertiary. $^{39}Ar/^{40}Ar$ age determinations and magnetostratigraphic studies carried out by many researchers (e.g. Courtillot *et al.*, 1986; Duncan & Pyle, 1988; Gallet *et al.*, 1989; Baksi & Farrar, 1991; Baksi, 1994), show a marked peak of activity at 65–67 Ma, within the 29R and, very subordinately, 29N magnetic chrons.

In spite of the monotonous sequence of the lava flows, sometimes recognized for several hundred kilometres (see Beane *et al.*, 1986), the Deccan Traps have been subdivided into several geochemical formations, following the approach of Najafi *et al.* (1981), based on the stratigraphic sampling of the lava sequence cropping out from Mahad to Mahableshwar, southeast of Bombay. After this attempt, several working groups have thoroughly studied the stratigraphic and geochemical features of the magmas of the Western Ghats, from Igatpuri, NW of Bombay, to Belgaum, at the southern end (e.g. Cox & Hawkesworth, 1985; Beane *et al.*, 1986; Devey & Lightfoot, 1986; Mahoney, 1988; Lightfoot *et al.*, 1990; Mitchell & Widdowson, 1991).

Geochemical differences throughout the basalt stratigraphy have been variously ascribed, apart from crystal fractionation, to

(1) upper-crustal contamination, in particular for the Bushe and part of the Poladpur Fms, which are characterized by high to very high $^{87}Sr/^{86}Sr$ initial ratios (>0·713 for the Bushe Fm; Devey & Lightfoot, 1986), and strong high field strength element (HFSE) negative anomalies in the mantle-normalized diagrams (e.g. Mahoney *et al.*, 1982; Cox & Hawkesworth, 1984, 1985);

(b) lithosphere–asthenosphere interaction in the petrogenesis of the most widespread Ambenali Fm (e.g. Lightfoot & Hawkesworth, 1988; Lightfoot *et al.*, 1990);

(3) lower-crust contamination to explain isotopic characteristics of both lower and upper formations (e.g. Jawhar to Khandala Fms; Peng *et al.*, 1994; Mahableshwar Fm.; Mahoney *et al.*, 1982; Lightfoot *et al.*, 1990).

In the southern part of the Western Ghats the geochemical formations distinguished so far [see Mahoney (1988) and Subbarao (1988) for further details] show a southwards overstep, possibly caused by a migration of the magmatic activity in response to the migration of the Indian plate northwards (see Devey & Lightfoot, 1986; Watts & Cox, 1989).

Comparatively, much less is known about the northern and northwestern part of the Deccan, in particular in the Kathiawar (Saurashtra) peninsula. Apart from some studies on post-Traps central complexes, e.g. Mt Girnar (Bose, 1973; Paul *et al.*, 1977; Sethna, 1988), no recent work is available on the exposed basalt sequence. On the other hand, detailed petrologic work has been carried out on boreholes in northeast Kathiawar (near Dhandhuka; West, 1958; Krishnamurthy & Cox, 1977), on the volcanics of the Pavagadh section [see also Tiwari (1966, 1972)] and on the Rajpipla area. This last is known from the literature also for a suite of potassic basalts interlayered with 'normal' tholeiites (Krishnamurthy & Cox, 1980; Mahoney *et al.*, 1985), and for post-Deccan alkaline rocks and carbonatites (e.g. Sethna, 1988; Gwalani *et al.*, 1992).

The aim of this paper is to present and discuss mineral chemical and geochemical data mainly for the basic volcanic products of the flood sequence of the Kathiawar peninsula, for the basaltic rocks of the Rajpipla area, and for the bimodal basic–acid volcanic sequence cropping out on the Pavagadh hill (Fig. 1a, b). The presence of primitive, high-MgO magma types and the observed compositional differences among the various Gujarat basalt groups are not seen in the Western Ghats and thus are of noteworthy significance in the geochemistry of the Deccan Traps.

GEOLOGICAL SETTING

The Deccan basalts in the Gujarat area overlie Mesozoic sediments made up of fluviodeltaic sandstones and shallow sea sediments, which, in turn, rest unconformably on the Archaean Aravalli craton (phyllites, quartzites and amphibolites; Biswas, 1982, 1987). A post-Deccan cover is present to the north, with shallow sea or continental facies, terminated by

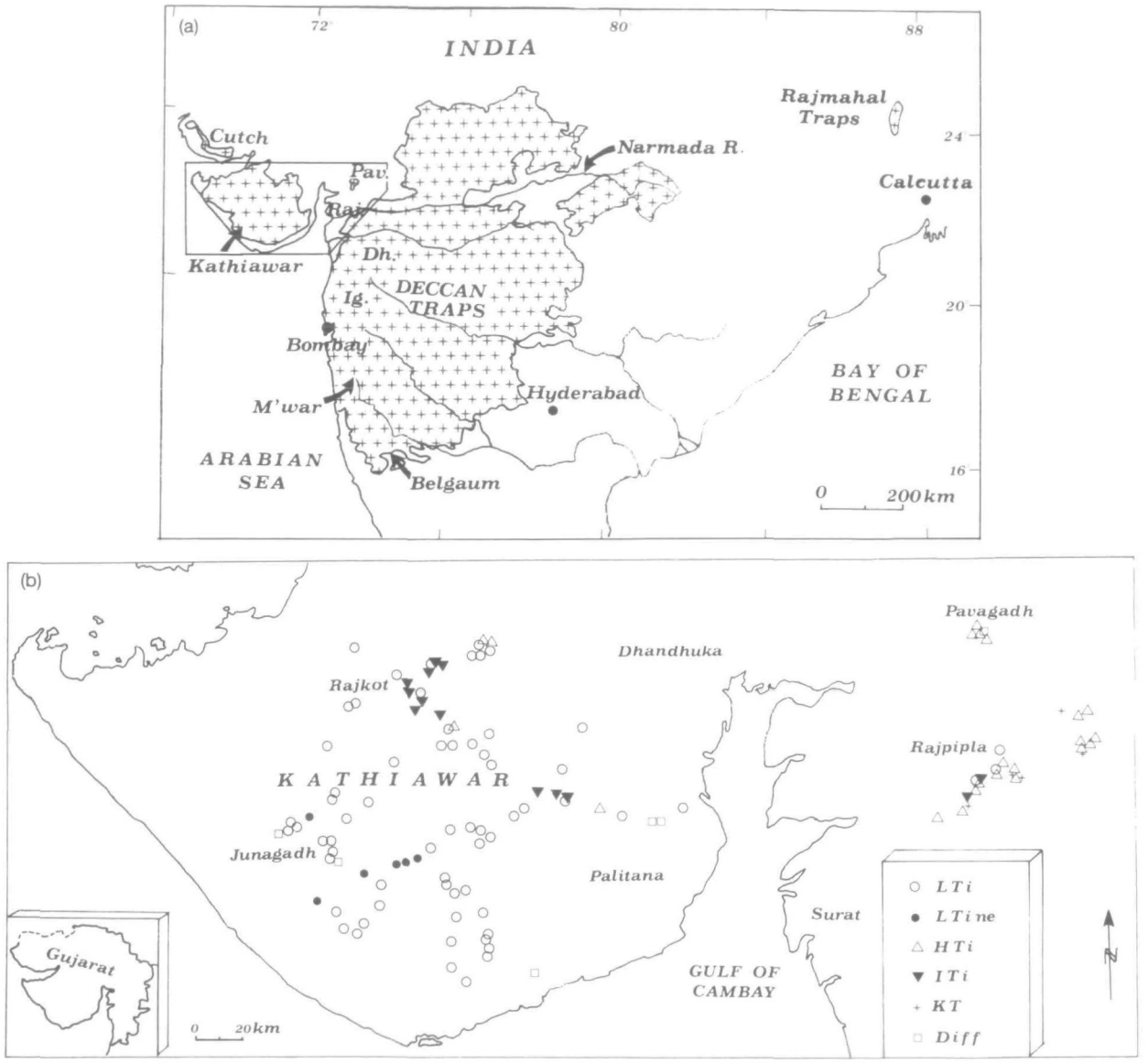

Fig. 1. (a) Sketch map of Central India. Dh., Dhule; Ig., Igatpuri; Pav., Pavagadh; Raj., Rajpipla; M'war, Mahableshwar. (b) Gujarat area, with sampling sites shown. The symbols indicate outcrops of the various basalt groups (see below).

the final Mio-Pliocene emergence (Biswas, 1982). The average thickness of the basalts in the Kathiawar peninsula has been inferred utilizing DSS (deep seismic sounding) data; it is thickest seawards (~1·5 km) and tends to be strongly reduced to the north (0·3 km; Kaila *et al.*, 1981). It is important to note that there are no exposed basalt sequences with such thicknesses in Kathiawar, which is morphologically an almost completely flat area. Moreover, in the northernmost occurrences of Kathiawar (Fig. 1b) no more than one or two flows rest upon pre-Deccan sandstones or directly upon the Precambrian basement. For these reasons, the stratigraphy of the area is difficult to elucidate, as are correlations within the recognized chemical types, in particular for the most widespread low-Ti group (see below). This is obviously unlike the clear stratigraphic relationships found in the basalts of the Western Ghats, owing to thick and generally well-exposed sections. However, basalts with distinct geochemical affinities are found interlayered in the northern part of the Kathiawar (north of Rajkot; Fig. 1b) and in the Rajpipla area, indicating at least some temporal interfingering between different groups of basaltic rocks.

A number of dykes are present in the southwestern part of Kathiawar, their regional strike (WNW–ESE) being broadly similar to that of the dykes in the Narmada–Tapti rift region (see Misra, 1981;

Hooper, 1990). There is, however, an intervening gap where the Cambay rift crosscuts the Narmada–Tapti region. In central Kathiawar the strike of the dykes is often random but in some cases the distribution follows a roughly radial pattern, and thus may be related to individual eruptive foci. The significance of the Cambay graben and of the Narmada–Son lineament is of interest in this context. The Narmada–Son lineament is currently interpreted as a dextral transcurrent fault, with an estimated displacement of 600–700 km, which probably was inactive during the eruption of the Deccan Traps, and was reactivated as a graben in very early post-Deccan times (Sen, 1991). The very abundant presence of rocks with a low-Ti affinity in Kathiawar (Fig. 1b), and their significant volumetric decrease in the northernmost Western Ghats seems to suggest a discontinuity in the lithospheric mantle.

GEOCHEMICAL CLASSIFICATION OF BASALT GROUPS

A set of 200 samples was analysed for major and trace elements; the analytical procedures are described in the Appendix. The basaltic rocks were first geochemically subdivided into two groups, because of the clear bimodality of the TiO_2 (Fig. 2a): the value of 1·8 wt % TiO_2 was used as the first-order discrimination between high- and low-Ti types. Within this first-order subdivision, further discrimination was made, taking into account the Nb contents (Fig. 2b) and K_2O/Na_2O ratio of the rocks (Fig. 2c). The most important characteristics of the various groups are summarized below:

The low-titanium (low-Ti) rocks form most of the outcrops of Kathiawar and range in composition from picrite basalt to andesite (Fig. 1b). These rocks are mostly tholeiitic, with olivine or quartz in their CIPW norms, and plot well within the subalkaline field of the total alkali–silica diagram (TAS; LeBas *et al.*, 1986; Fig. 3). The low-Ti rocks are also characterized by low Nb contents (<10–12 p.p.m., 80 out of 90 basalts have <9 p.p.m.), together with low K_2O/Na_2O, low Zr/Y (av. 3·7 ± 0·6), and Ti/Y (281 ± 53) ratios. The values of the latter ratios are completely within conventional limits used to distinguish Gondwana low-Ti CFBs (Zr/Y < 6 and

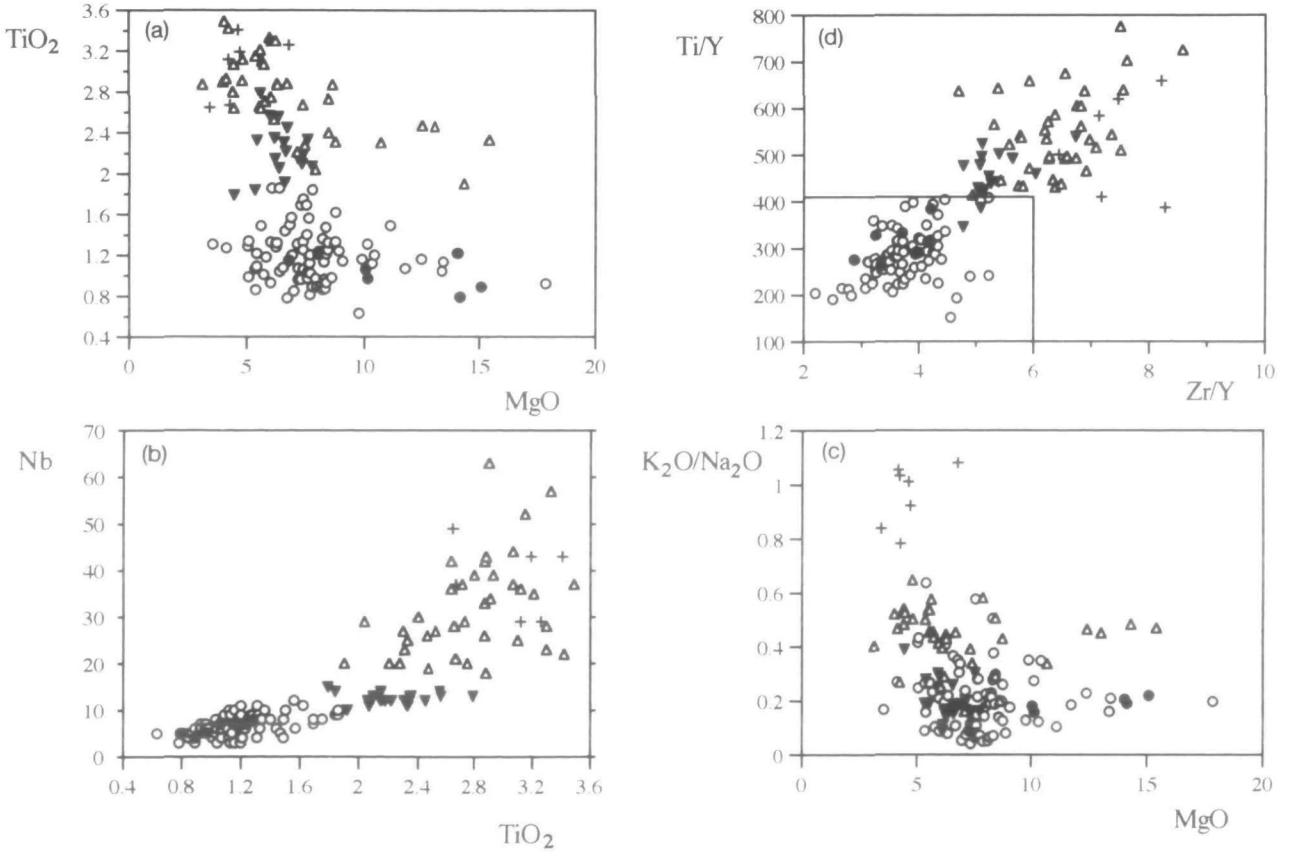

Fig. 2. Discrimination diagrams. (a) MgO–TiO_2; (b) TiO_2–Nb; (c) MgO vs K_2O/Na_2O; (d) Zr/Y vs Ti/Y; in this diagram the lines represent the limits of low-Ti basalts as given by Erlank *et al.* (1988). +, KT, △, high-Ti; ▼, I-Ti; ○, low-Ti; ●, low-Ti ne-norm.

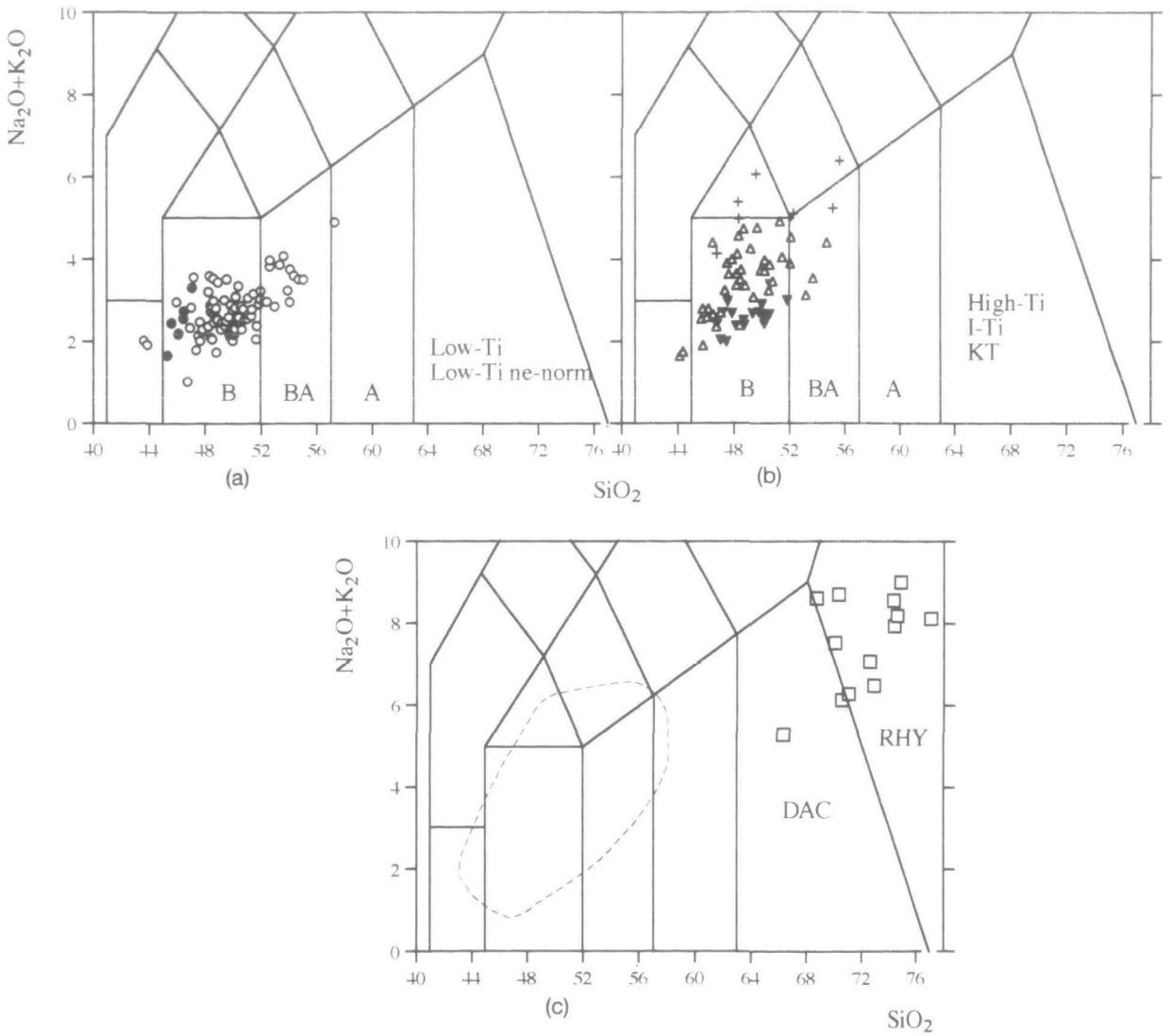

Fig. 3. Total alkali–silica diagrams. (a) Low-Ti (open circles) and ne-normative low-Ti (full circles); (b) I-Ti (reversed, filled triangles), high-Ti (open triangles), KT (crosses); (c) differentiated rocks.

Ti/Y<410; Erlank *et al.*, 1988; Fig. 2d). Some picrites and basalts with low-Ti affinities have only a few percent hypersthene in their CIPW norms, or are even nepheline-normative. They also contain a distinct type of clinopyroxene (see below).

The rocks with TiO_2 >1·8 wt% have been subdivided into three groups:

(1) a high-Ti group, ranging in composition from picrite basalt to basaltic andesite, which is slightly richer in K than the low-Ti group (higher average K_2O/Na_2O ratios) and much higher in incompatible trace element contents, in particular Nb, even in the picritic rocks (Nb>19 p.p.m.; Fig. 2b, c). The basalts of the Dhandhuka borehole (Krishnamurthy & Cox, 1977) belong to this group.

(2) A potassium-rich tholeiitic (KT) group is made up of slightly more alkalic rocks and crops out near Rajpipla. This group is easily distinguished from the high-Ti rocks by the higher K_2O/Na_2O ratio (close to unity; Fig. 2c), but has otherwise broadly similar geochemical features.

(3) An intermediate-Ti rock group (I-Ti), which is mostly made up of basalts, also has distinctly lower Nb contents (10–15 p.p.m.; Fig. 2b, c) and K_2O/Na_2O than high-Ti rocks. The Nb (and TiO_2) contents of this last group are, however, distinctly higher than those of the low-Ti rocks, as are their Ti/Y and Zr/Y ratios (Fig. 2d). The substantially lower Nb and K_2O contents of the I-Ti group compared with the high-Ti picrites and basalts preclude fractional crystallization as a simple explanation of the

Table 1: Key discrimination criteria to define the basaltic groups of Gujarat

TiO_2 (wt%)		Nb (p.p.m.)	K_2O/Na_2O	Petrogr. types	Ca-rich px
<1·8	Low-Ti	<12	0·20±0·06	P, B, BA, A	augite
	Low-Ti ne-norm			P, B	salite
>1·8	I-Ti	10<Nb<15	0·19±0·06	B	augite
	High-Ti	>19	0·44±0·05	P, B, BA	diopside, salite
	KT		>0·8	B, BA	n.a.

P, picrite basalts; B, basalts; BA, basaltic andesites; A, 'andesites'; n.a., not analysed.

observed array of compositions. Similarly, no simple genetic relationships are likely between the I-Ti and low-Ti basalts (see also major and trace elements).

Some of the most important geochemical characters of the groups of broadly basaltic rocks are given in Table 1, but we note also the presence of strongly differentiated rocks (dacites and rhyolites; see Fig. 3c).

PETROGRAPHY

The investigated rocks range from picrite basalts to rhyolites, and show petrographic and mineral chemical characters which easily help to distinguish the geochemical groups defined above.

Picrite basalts

Picrite basalts have textures from almost completely aphyric, with rare olivine phenocrysts set in a very fine-grained intersertal groundmass, to porphyritic and sometimes doleritic. The low-Ti picrites are characterized by euhedral to subhedral olivine phenocrysts and microphenocrysts, with euhedral chrome spinel inclusions; plagioclase is not always present as a phenocryst but is ubiquitous in the groundmass; clinopyroxene is never found as a phenocryst, but only as a pseudophitic or intergranular phase in the mesostasis; rare and very late microlites of opaque oxides are observed. This picrite type is widespread only in Kathiawar. The nepheline-normative low-Ti picrites are very similar to the subalkaline low-Ti analogues, except for the presence of late and pseudophitic pale-violet (Ti-rich) clinopyroxene. The picrite basalts of the high-Ti group, grading to ankaramite or three-phenocryst basalt, are made up of olivine (± chrome spinel), subordinate colourless to light green clinopyroxene phenocrysts (always crystallized after olivine), and slightly lesser amounts of plagioclase, still frequently enclosed in clinopyroxene; the groundmass has very abundant opaque grains, thus giving a darker appearance to the rocks. This type is absent from most of Kathiawar, excluding its northern part, but is common in the Pavagadh and Rajpipla sectors. West (1958) presented a very detailed study of the three-phenocryst basalts and picrite basalts (and basalts as well) which were found in the boreholes of Botad, Dhandhuka and Wadhwan junction, located in northeastern Kathiawar (Fig. 1a). The high-Ti picrites of this study show strikingly similar petrographic characters.

Basalts

Basalts show textures varying from intersertal to pseudophitic or porphyritic in the low-Ti and I-Ti basalts. High-Ti and KT basalts are generally weakly (plag + cpx ± olivine)-phyric, and are mostly found with pilotaxitic textures. Olivine is minor or absent and plagioclase is the dominant phenocryst, only later joined by clinopyroxene and interstitial oxides. These latter have been never found as phenocrysts. Two major petrographic types were distinguished, taking into account the relative abundance of pyroxene phenocrysts and groundmass opaque oxides. Olivine is observed as a phenocryst or microlitic phase in many rocks of all the geochemical groups, regardless of the SiO_2 saturation of the host rocks; on the other hand, rare pigeonite has been found only in some low-Ti basalts, very rarely enclosed in augite (D146), or within the late-crystallized intersertal or pseudophitic mesostasis; interstitial amphibole, granophyric alkali feldspar and quartz, and sometimes also glass (of rhyolitic composition), are sporadically observed.

Basaltic andesites and andesites

Basaltic andesites and the very rare (tholeiitic) andesites (the latter with a low-Ti affinity) have a doleritic texture, with significant amounts of granophyric or glassy groundmass (the latter being invariably rhyolitic in composition). Moreover, they have more frequent, but not abundant opaque phenocrysts, in addition to Na-labradoritic to andesinic plagioclase and (light green) pyroxenes richer in Fe than less differentiated rocks. Like the basalts, these lithotypes have been found over the whole Gujarat area.

Dacites and rhyolites

Dacites and rhyolites, particularly rhyolites, are more abundant than the intermediate rocks (Fig. 3). Their occurrence is mainly concentrated in eastern Kathiawar and in the Pavagadh sequence (up to 200 m of rhyolites), but they also occur in the region of the Girnar complex (Junagadh); some of them (D21) belong to the post-Deccan intrusions of Kathiawar. The dacite D66 (Table 2) has a weakly porphyritic texture with phenocrysts of labradorite to oligoclase feldspar, low-Ti–high-Fe augite, pigeonite and magnetite, set in a strongly altered granophyric mesostasis.

Pitchstones and pyroclastics are the most frequent lithologies of the rhyolitic rocks. They are more or less porphyritic, with sparse phenocrysts of andesine to anorthoclase feldspar, Ca-rich pyroxenes, sporadic fayalitic olivine, pigeonite, orthopyroxene and opaque oxide set in a glassy matrix. Tiny zircon crystals are very rarely observed. Devitrification is widespread, and usually the rocks are highly altered, precluding a more thorough knowledge of the parageneses.

CHEMICAL VARIATIONS OF THE MINERAL PHASES

A large number of mineral chemical data on selected rocks have been obtained utilizing two different microprobes. Details of the analytical techniques are given in the Appendix. Trivalent iron contents have been calculated using the algorithm of Papike *et al.* (1974) for pyroxenes and amphiboles, and following Carmichael (1967) for oxides.

Pyroxenes

A wide compositional range is observed for the pyroxenes of the Gujarat rocks, generally broader than that observed in other parts of the Deccan Traps (cf. Western Ghats; Sen, 1986). Data are given in Table 2.

First-order differences in chemistry and cationic substitutions are observed (Figs 4 and 5). Ca-rich clinopyroxene compositions of low-Ti rocks plot well within the augite–Fe-augite field and show a clear tendency to Fe enrichment and Ca depletion from core to rim and with increasing differentiation. The *mg*-number [$Mg/(Mg+Fe^{2+})$] varies from 0·82 to 0·36; reverse zoning was never noted. Sometimes, subcalcic augites have been found; available data on similar rocks (e.g. Mellini *et al.*, 1988; Brotzu *et al.*, 1992) allowed the researchers to interpret these compositions as probable metastable phases which exsolve two pyroxenes in the subsolidus.

The calculated Fe^{3+} contents of these low-Ti-related pyroxenes are low, and confirm relatively reduced conditions of crystallization. Also, Al^{VI}, Al^{IV}, Na and Ti (Fig. 5) are very low (the last element very rarely exceeding 1 wt % as oxide), and tend to remain constant or even decrease with decreasing Mg. Cr is invariably below the detection limits, confirming that these pyroxenes grew from already differentiated magmas. No significant variations in the pyroxene chemistry were observed for the low-Ti rocks from Rajpipla to the Kathiawar peninsula, thus suggesting remarkably similar conditions of crystallization over several hundred kilometres.

Some low-Ti rocks show very small amounts of pigeonite, sometimes found also in the groundmass of picrites (D130) as a very late phase along with quartz. The compositional range of pigeonites, from picrite basalt to the D66 dacite (which have all the petrographic characters of the low-Ti rocks) is from $Ca_9Mg_{69}Fe_{22}$ to $Ca_9Mg_{42}Fe_{48}$ (Fig. 4). The equilibration temperatures obtained using the pigeonite geothermometer of Ishii (1976) range from 1156 to 1017°C, with the highest values found in picrites and basalts. Similar results (1160–1000°C) have been obtained utilizing the two-pyroxene thermometers of Lindsley (1983) and Andersen & Lindsley (1988).

The clinopyroxenes of the nepheline-normative low-Ti rocks are diopsides to salites which plot parallel to the Di–Hd join (Fig. 4a). They have higher Ti and Al contents (up to 2·78 and 5·26 wt %, respectively) compared with the values of the low-Ti pyroxenes, even though they are very late in crystallization. In this group pigeonite is absent, but a unusual suite of subcalcic diopsides was found as rounded relicts within Cr–Al-spinels, both included in low-pressure, 'Ca-rich' olivine or, less frequently, outside (sample D56; Fig. 4). Variations of the chemistry of these subcalcic diopsides are large both for Ca and minor elements Cr, Na, Ti and Al (Table 2); moreover, there is a clear tendency for these pyroxenes to have high Al^{VI}/Al^{IV} ratios (up to 0·4), with respect to the late-crystallized salites. A likely explanation for the genesis of this suite is the

Table 2: Selected analyses of pyroxenes

	High-Ti											I-Ti				Low-Ti				
	D82	D82	D81	D81	D81	D44	D44	D97	D97	D79	D79	D42	D42	D121	D121	D57	D57	D56	D56	D58
	E	L	E	L	L	E	L	E	L	E	L	E	L	E	L	L	L	L	L	L
SiO_2	50·56	45·69	49·96	50·45	48·24	50·52	44·28	52·46	48·13	47·71	48·20	52·10	51·06	52·89	49·58	51·29	51·49	47·91	47·96	46·96
TiO_2	1·33	2·94	1·01	1·55	2·23	0·62	3·58	0·65	3·03	2·52	2·64	0·76	1·29	0·83	1·89	0·63	1·43	1·88	2·22	2·78
Al_2O_3	3·44	7·21	3·64	1·99	2·66	2·99	6·84	2·31	4·02	4·24	4·03	2·49	1·97	2·41	2·56	4·21	1·57	5·13	3·34	3·39
FeO	6·02	8·06	5·37	10·83	15·80	4·41	9·76	4·27	10·57	9·37	9·66	6·98	12·38	6·88	13·44	6·09	9·78	10·73	14·43	17·70
MnO	0·13	0·17	0·13	0·34	0·39	0·05	0·15	0·11	0·31	0·13	0·14	0·18	0·31	0·18	0·26	0·11	0·31	0·18	0·15	0·38
MgO	15·69	12·89	15·96	13·31	8·55	16·37	11·65	16·45	13·01	13·39	13·40	16·79	13·80	17·98	14·47	15·05	13·88	13·30	10·89	8·25
CaO	21·94	21·59	22·38	21·02	20·84	23·45	22·29	22·42	20·04	21·38	20·86	19·99	18·75	18·54	17·18	22·00	20·92	19·52	19·97	19·68
Na_2O	0·19	0·35	0·18	0·30	0·72	0·22	0·38	0·23	0·37	0·40	0·41	0·29	0·22	0·20	0·23	0·33	0·38	0·46	0·53	0·51
Cr_2O_3	0·17	0·34	0·53			0·53	0·10	1·01		0·02		0·04								
Total	99·47	99·24	99·16	99·79	99·43	99·16	99·03	99·91	99·48	99·16	99·34	99·62	99·78	99·91	99·61	99·71	99·76	99·11	99·49	99·65
Ca	45·2	47·0	45·8	43·6	45·9	47·2	48·2	46·0	43·0	45·1	44·2	40·8	38·0	37·8	35·8	46·0	43·5	41·9	42·9	43·5
Mg	44·9	39·0	45·4	38·4	26·2	45·8	35·1	47·0	38·8	39·3	39·5	47·7	39·0	51·0	41·9	43·8	40·1	39·8	32·6	25·4
Fe*	9·7	13·7	8·6	17·5	27·2	6·9	16·5	6·8	17·7	15·4	16·0	11·1	22·5	10·9	21·8	9·9	15·9	18·0	24·2	30·5

	Low-Ti															DAC			
	D56	D56	D56	D60	D60	D130	D130	D208	D208	D105	D105	D105	D211	D211	D73	D73	D66	D66	D66	D66
	Sub-Di	Sub-Di	Sub-Di	L	L	L	Pig-L	L	Pig-L	E	L	L	E	L	L	L	E	L	Pig-E	Pig-L
SiO_2	50·91	48·82	51·50	52·28	50·33	51·67	53·39	51·30	51·52	52·61	50·69	48·83	50·67	50·03	50·61	49·76	50·02	51·62	51·52	48·75
TiO_2	0·18	0·34	0·72	0·68	0·95	0·74	0·52	0·23	0·15	0·43	0·89	0·66	0·73		0·80	0·65	0·63	0·67	0·30	0·49
Al_2O_3	4·26	7·85	3·76	1·78	1·48	2·57	1·45	2·18	1·15	1·79	1·37	1·04	2·22	1·13	1·72	1·45	1·94	1·50	0·63	0·70
FeO	5·00	6·05	5·41	8·57	18·27	9·86	15·43	7·93	21·21	7·85	17·42	25·73	12·87	18·13	14·62	20·57	14·98	16·02	23·75	28·91
MnO	0·12	0·04	0·16	0·25	0·52	0·35	0·43	0·23	0·44	0·22	0·37	0·62	0·34	0·47	0·39	0·54	0·53	0·37	1·07	0·67
MgO	19·55	21·98	21·12	15·89	13·04	15·85	23·63	17·86	19·87	17·74	12·44	7·99	14·91	11·53	12·72	11·66	13·93	12·15	18·37	15·01
CaO	17·70	12·57	15·30	19·90	14·72	18·49	4·26	19·30	4·98	18·53	16·81	15·21	17·48	17·36	18·80	15·16	17·26	16·59	4·62	4·08
Na_2O	0·22	0·23	0·29	0·19	0·16	0·14		0·20	0·05	0·13	0·11	0·01	0·10	0·10	0·20	0·13	0·17	0·63	0·02	
Cr_2O_3	1·31	0·94	1·01	0·10		0·10				0·15										
Total	99·25	98·82	99·27	99·64	99·47	99·77	99·11	99·23	99·37	99·45	100·10	100·09	99·32	98·75	99·86	99·92	99·46	99·55	100·28	98·61
Ca	36·2	26·2	31·2	40·7	31·0	38·1	8·6	38·2	10·1	37·4	35·0	32·4	36·0	36·2	39·0	31·7	35·4	35·8	9·3	8·5
Mg	55·6	63·8	59·9	45·2	38·2	45·5	66·4	49·2	55·8	49·8	36·1	23·7	42·7	33·5	36·7	33·9	39·8	36·5	51·6	43·5
Fe*	8·0	9·9	8·6	13·7	30·0	15·9	24·3	12·3	33·4	12·4	28·3	42·8	20·7	29·5	23·7	33·5	24·0	27·0	37·4	47·0

E, early; L, late; Fe*, Fe+Mn; Sub-Di, subcalcic diopside; Pig, pigeonite.

JOURNAL OF PETROLOGY VOLUME 36 NUMBER 5 OCTOBER 1995

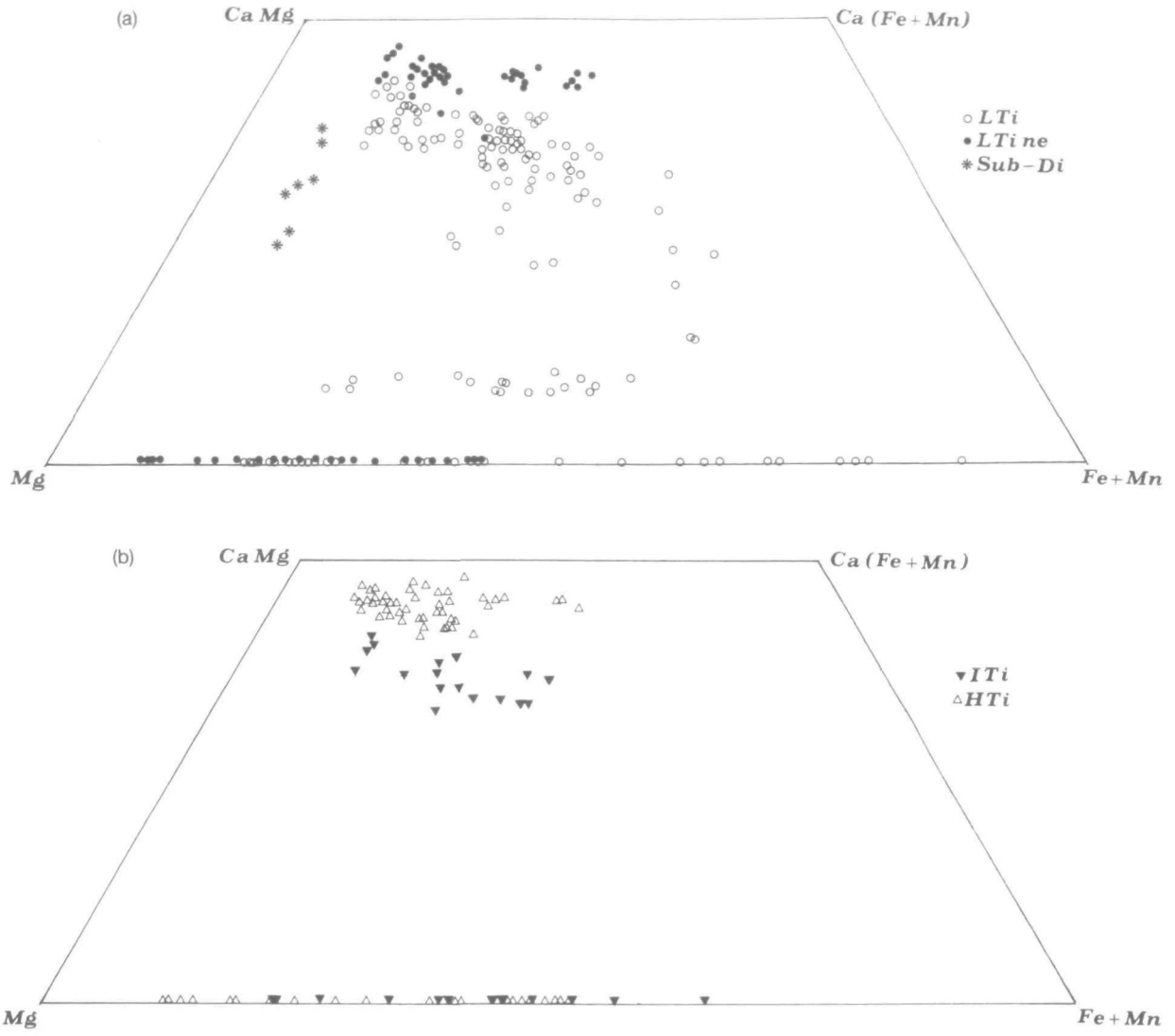

Fig. 4. Pyroxene and olivine compositions as projected in the Ca–Mg–(Fe + Mn) diagram. (a) Low-Ti rocks: asterisks indicate subcalcic diopsides in the sample D56 (ne-normative low-Ti); (b) I-Ti and high-Ti rocks.

crystallization in a higher-pressure and -temperature environment, followed by the low-pressure paragenesis and crystallization order (ol + plag + Ti-salite + Ti-mt).

The pyroxenes of the high-Ti suite range from diopsides to Fe-salites; *mg*-numbers range from 0·87 to 0·49; maximum TiO_2 and Al_2O_3 contents are 3·7 and 7 wt %, respectively. Na_2O contents, on the other hand, tend to be low, although they are higher than for low-Ti rocks, reaching values up to 0·8 wt %. It is interesting to note that the most Mg-rich pyroxenes have been found in rocks of the high-Ti suite, thus confirming the earlier appearance of this phase in these slightly more alkali-rich rocks.

The Ca-rich pyroxenes of the rocks with I-Ti affinity are mostly augites and show relatively restricted compositional variations (Fig. 4), with *mg*-number ranging from 0·81 to 0·59. The most important distinction between these pyroxenes and those of the low-Ti rocks is the greater increase in the former of Ti (Fig. 5) and, consequently Al, from early to late crystallization stage. Na_2O is also very slightly higher (0·16–0·57 wt %).

In summary, even if the pyroxenes of both the low-Ti and I-Ti groups are augites (and Fe-augites) there are clear and strong differences in their TiO_2, Al_2O_3 and Na_2O contents, and there is little doubt that they reflect different chemical conditions of crystallization. On the other hand, more alkali-rich rocks (the nepheline normative low-Ti and the high-Ti rocks) have the most Ca- and Ti-rich pyroxenes, and this is so regardless of the TiO_2 content of the

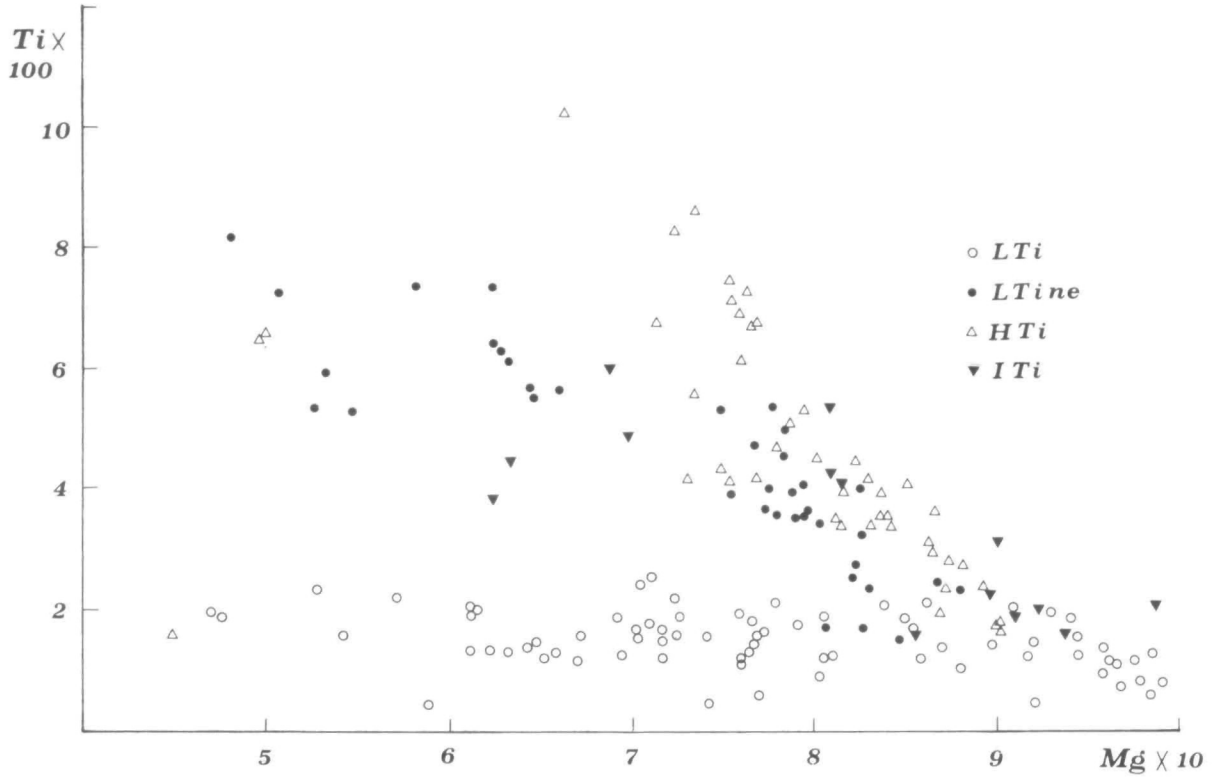

Fig. 5. Ti–Mg diagram for early- and late-crystallized Ca-rich pyroxenes of the various groups.

host rocks. However, the magnitude of the Ti enrichment is higher in the high Ti rocks (Fig. 5), when compared with the nepheline-normative low-Ti analogues.

Olivine

Olivine is a common phase both as coarse-grained euhedral to subhedral phenocrysts (in some cases skeletal, or rarely with a weak kink banding) and as microlites in the groundmass, and without reaction rims involving Ca-poor pyroxenes. A wide and continuous compositional range has been observed (Table 3 and Fig. 4), from Fo_{91} to Fo_{11}. No compositional difference was noted among the various basalt groups. MnO ranges from 0·05 to 1·8% and CaO from 0·2 to 0·5%, with the highest values found in the most Fe-rich varieties.

When compared with the host rock *mg*-number, the olivines tend to be richer in Fe than expected from the empirical relationship of Roeder & Emslie (1970), particularly for the picrite varieties. This indicates a relatively slow and quasi-equilibrium crystallization in many samples. This feature has already been recognized by Beane & Hooper (1988) in their study on picrite basalts in the central Deccan; they concluded that picrites are crystal-enriched versions of normal basalts. In the Gujarat picrite rocks, relatively Fe-rich olivines enclose Cr-spinels and sometimes are found as intergrowths with plagioclase. Only in a rhyolite (D89; Pavagadh) have Fe-rich olivines been found (Fo_{28}; Table 3).

Feldspars

Feldspars of the two main groups show clear differences in the evolution trend, although these are more subtle than those of the pyroxenes. Plagioclases from low-Ti rocks range from An_{82} to An_{15} (Fig. 6) and only a very slight orthoclase enrichment is seen, as a consequence of the very low K_2O content of the host magmas. Na-sanidine was positively recognized only in the late-stage, fine-grained mesostasis of a dolerite (D208; Rajpipla). A much broader range of compositions was observed in the rocks of the high-Ti and I-Ti rocks, from bytownite (An_{80}) through anorthoclase, found in the groundmass of many high-Ti basalts and picrites, to sanidine (Fig. 6, Table 4). The overall increase in K_2O contents is evident, in particular for the late-crystallized feldspars (Fig. 6), and the trend is much more like that of mildly alkaline rock suites, when compared with that of the low-Ti rocks. Plagioclase equilibration temperatures were obtained using the calibration of Glazner

Table 3: Selected analyses of olivine

	High-Ti						I-Ti		Low-Ti				
	D97	D97	D81	D79	D79	D68	D42	D42	D56	D56	D57	D57	D101
	E	L	E	E	L	L	E	L	E	L	E	L	E
SiO_2	40·50	37·80	39·90	35·40	34·56	32·83	38·72	38·90	40·87	38·19	38·90	36·63	38·91
FeO	11·48	25·41	14·16	38·16	41·96	49·54	20·33	20·91	8·84	19·05	23·02	31·55	18·03
MnO	0·19	0·48	0·20	0·49	0·73	0·88	0·31	0·30	0·07	0·23	0·35	0·52	0·23
MgO	47·30	36·00	45·21	25·60	22·21	15·49	40·11	40·07	49·18	40·30	38·78	30·72	41·63
CaO	0·37	0·33	0·34	0·29	0·26	0·37	0·37	0·31	0·33	0·38	0·31	0·36	0·37
Total	99·84	100·02	99·81	99·94	99·72	99·11	99·84	100·49	99·29	98·15	101·36	99·78	99·17
Fo	88	72	85	54	49	36	78	77	91	79	75	63	65

	Low-Ti									Rhy
	D60	D130	D208	D208	D47	D47	D47	D45	D45	D89
	E	E	rol	L	E	L	L	E	L	E
SiO_2	39·18	38·90	35·88	34·73	38·53	35·86	30·70	39·00	33·01	32·46
FeO	17·53	19·49	35·16	41·42	21·48	35·53	63·67	21·69	54·64	54·59
MnO	0·24	0·32	0·44	0·48	0·39	0·47	1·02	0·33	1·15	1·71
MgO	42·24	40·93	28·08	22·93	39·14	27·62	4·51	40·07	12·60	11·75
CaO	0·31	0·25	0·20	0·24	0·40	0·39	0·53	0·37	0·37	0·29
Total	99·50	99·89	99·76	99·80	99·94	99·87	100·43	101·46	101·77	100·80
Fo	81	79	59	50	76	58	11	77	29	28

E, early; L, late; Fo, forsterite mol%.

(1984). Average maximum temperatures are 1204 ± 30°C for picrite basalts, 1200 ± 30°C for basalts, and 1125 ± 45°C for basaltic andesites (Melluso, 1992). The values are slightly higher than those obtained by pyroxene thermometry (see above) and so are in excellent agreement with all the petrographic observations. The similar values for picrites and basalts are matched by the relative constancy of the An contents of plagioclase, suggesting similar liquidus temperatures for this phase, regardless of the degree of differentiation.

Oxides

At least two generations of oxides are found in the Gujarat rocks: the first is represented by Cr- and Al-bearing spinels found enclosed in olivine or, rarely, in plagioclase or as microphenocrysts; the second is the late-crystallized suite of Ti-magnetites and ilmenites typical of subalkaline rocks. Minor sulphide (mostly chalcopyrite) and rare groundmass pseudobrookite have been observed.

The spinels found enclosed in olivine range from Al-spinel to Cr-bearing Ti-magnetite (up to 50 mol% ulvöspinel); no significant variations related to the chemistry of the host olivines (as Mg-low as Fo_{57}) and to the geochemical affinity of the host rocks are observed (Table 5 and Fig. 7). The general core-to-rim and within-sample variations of these spinels are related to three main cationic substitutions: $Mg \rightarrow Fe^{2+}$, $Al \rightarrow Cr$ and $Al + Cr \rightarrow Fe^{3+} + Ti$ (Fig. 7; Table 5). The differences between early and groundmass spinels are mainly due to the absence of Cr and the low Al contents in the latter (up to 6 wt% Al_2O_3, but most data cluster around 2%). Similar variations in the spinel chemistry are

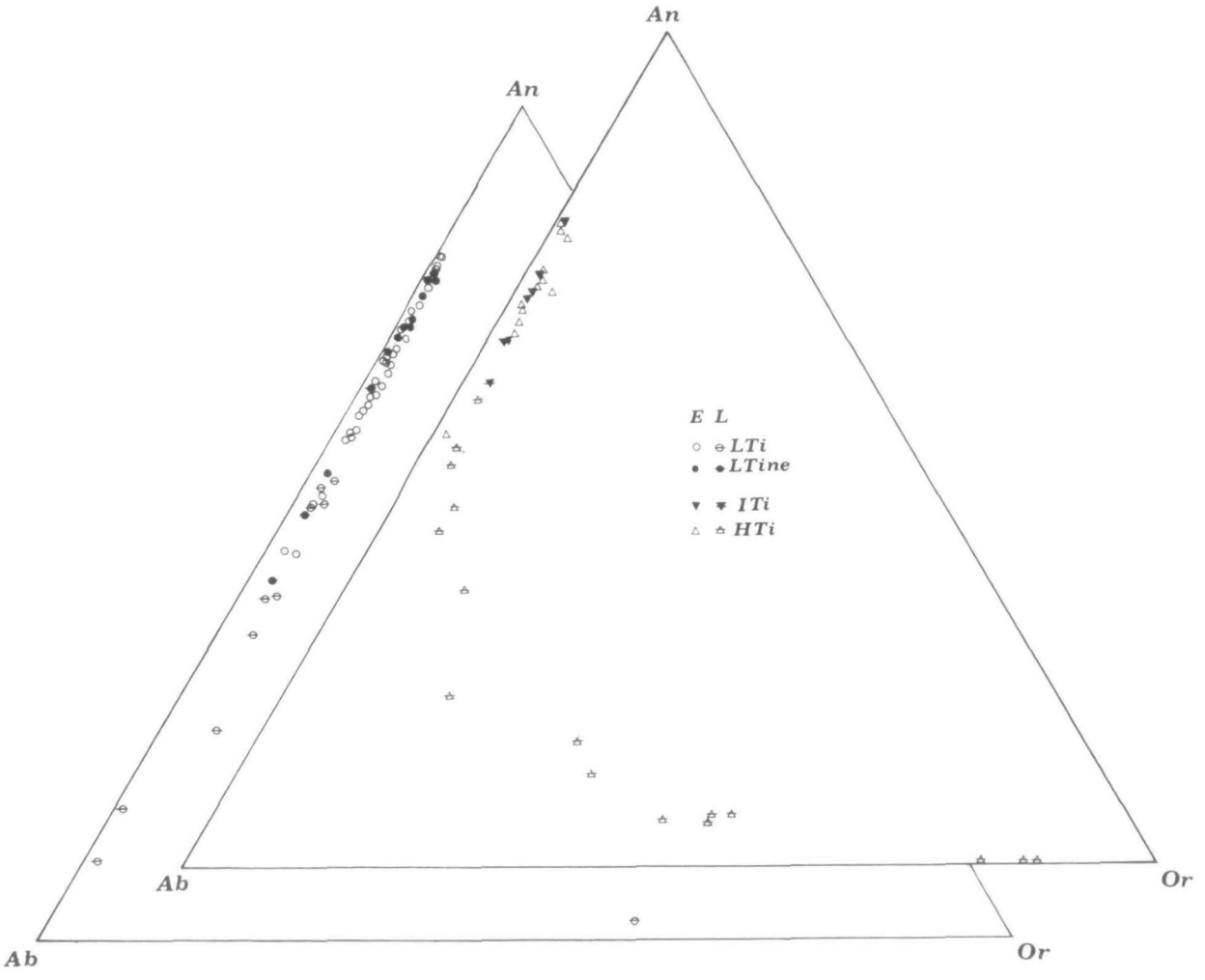

Fig. 6. Feldspar diagrams for the basic rocks of Gujarat. E, early; L, late.

observed in many other rock suites elsewhere (see Ridley, 1977; Allan *et al.*, 1988; Cawthorn *et al.*, 1991), but only very few data on Deccan Cr-spinels are available in the literature (see Krishnamurthy & Cox, 1977; Sen, 1986).

Groundmass Ti-magnetite and ilmenite pairs showed a large range of equilibration temperatures, from ~1170 to 700° C (Fig. 8a), and five orders of magnitude in the oxygen fugacity, according to the geo-thermobarometers of Buddington & Lindsley (1964) and Andersen & Lindsley (1988). The f_{O_2} and T values are clustered between the nickel–nickel oxide (NNO) and wüstite–magnetite (WM) buffers. Most high-Ti rocks plot above the quartz–fayalite–magnetite (QFM) buffer, and low-Ti rocks plot below. The nepheline-normative low-Ti rocks show different behaviour with respect to the main low-Ti trend, being scattered both above and below the QFM buffer. The equilibration temperatures and oxygen fugacities of the I-Ti rock D121 plot below the QFM buffer, as in the low-Ti rocks. The f_{O_2} and T values obtained by Sethna & Sethna (1988) on magnetite–ilmenite pairs in rocks cropping out in the Igatpuri area are substantially similar, thus suggesting broad uniformity of oxidation conditions in a large part of the Deccan lavas.

A small number of pseudobrookites (Table 6 and Fig. 8b) were analysed in the groundmass of three rocks. The occurrence of this phase (in high-Ti and in nepheline-normative low-Ti rocks) possibly suggests high oxidation conditions in the latest crystallization stages.

Other phases

Very rare amphiboles have been observed in some low-Ti basalts. They are very late crystallizing phases, growing sometimes as rims on clinopyroxene

Table 4: Selected analyses of feldspars

	High-Ti										I-Ti			Low-Ti	
	D81	D81	D81	D44	D44	D97	D97	D79	D79	D79	D42	D42	D121	D108	D57
	E	L	L	E	L	E	L	E	L	L	E	L	E	E	E
SiO_2	49·11	55·57	65·09	48·59	51·10	50·07	56·29	50·40	61·55	63·96	50·08	53·15	51·08	48·09	47·66
Al_2O_3	32·02	27·78	19·88	32·52	30·61	31·12	26·64	31·11	22·34	19·53	31·28	28·97	30·94	32·62	32·47
FeO	0·58	0·46	0·32	0·44	0·57	1·03	0·92	0·59	1·41	1·20	0·56	1·09	0·47	0·59	1·16
CaO	14·94	9·69	1·16	15·40	13·38	13·93	8·84	13·96	4·29	1·09	14·32	11·55	13·65	15·75	15·72
Na_2O	2·81	5·67	5·60	2·69	3·69	3·33	5·96	3 15	7·12	5·00	3·19	4·55	3·56	2·40	2·24
K_2O	0·21	0·59	7·91	0·27	0·21	0·30	1·07	0·64	2·86	8·61	0·18	0·45	0·25	0·06	0·22
Total	99·67	99·76	99·96	99·91	99·56	99·78	99·72	99·85	99·57	99·39	99·61	99·76	99·95	99·51	99·47
An	73·7	46·9	5·6	74·8	65·9	68·6	42·3	68·4	20·8	5·3	70·5	56·8	66·9	76·4	78·5
Ab	25·1	49·7	48·9	23·6	32·9	29·6	51·6	27·9	62·6	44·4	28·4	40·5	31·6	21·1	20·2
Or	1·2	3·4	45·5	1·5	1·2	1·8	6·1	3·7	16·5	50·3	1·0	2·6	1·5	2·6	1·3

	Low-Ti														DAC
	D56	D56	D58	D60	D60	D130	D208	D208	D105	D105	D211	D211	D73	D73	D66
	E	L	L	E	L	L	E	L	E	L	E	L	E	L	L
SiO_2	48·06	49·23	50·63	49·59	51·94	50·23	49·16	64·98	52·59	57·58	51·06	57·21	51·03	64·16	65·92
Al_2O_3	32·61	31·69	31·04	31·93	30·09	30·98	31·72	18·93	29·73	26·06	30·44	26·70	30·55	22·02	20·94
FeO	0·79	0·72	0·73	0·39	0·70	1·11	0·82	0·70	0·71	0·56	0·81	0·39	0·79	0·32	0·40
CaO	15·69	14·58	13·83	14·85	12·82	14·06	14·73	0·52	12·18	8·23	13·27	8·63	13·29	3·13	1·89
Na_2O	2·59	3·13	3·47	2·92	3·97	3·22	2·98	4·45	4 46	6·58	3·69	6·36	3·69	9·77	10·50
K_2O	0·11	0·21	0·17	0·12	0·24	0·18	0·08	10·00	0·25	0·49	0·18	0·42	0·26	0·13	0·11
Total	99·85	99·56	99·87	99·80	99·76	99·78	99·49	99·58	99·92	99·50	99·45	99·71	99·61	99·53	99·76
An	76·5	71·1	68·1	73·2	63·2	69·9	72·9	2·5	59·3	39·7	65·8	41·8	65·5	14·9	9·0
Ab	22·9	27·6	30·9	26·1	35·4	29·0	26·7	39·3	39·3	57·5	33·1	55·8	32·9	84·3	90·4
Or	0·6	1·2	1·0	0·7	1·4	1·1	0·5	58·1	1·4	2·8	1·1	2·4	1·5	0·7	0·6

E, early; L, late; Ab, An, Or in mol %.

or with quartz in the granophyric mesostasis. The amphibole composition is Fe-edenitic hornblende and Fe-hornblende [following Leake (1978)]. These minerals are low in Al, alkalis and Ti (Table 6), and thus are clearly derived from residual subalkaline magmas. Fe-phlogopite has been found as a miarolitic phase in the basalt D79 (high-Ti) at Pavagadh; its composition is uniform, very magnesian, and Ti rich (Table 6).

MAJOR AND TRACE ELEMENT VARIATIONS

Within the framework of the classification scheme of Table 1 and Fig. 2, the various groups show significant trends in major and trace elements, which are broadly compatible with crystal fractionation of the observed phases; in particular, looking at the diagrams of Fig. 9, it may be observed that CaO,

Table 5: Selected analyses of spinels

	High-Ti							I-Ti		Low-Ti				
	D82	D82	D97	D97	D97	D44	D79	D121	D42	D56	D56	D56	D56	D56
	E	L	C	R	L	L	L	L	L	E	E	E	L	L
TiO_2	4·93	21·88	1·54	3·83	16·87	23·53	15·54	26·77	23·28	0·18	0·21	6·39	17·44	21·75
Al_2O_3	15·45	1·98	11·27	7·92	1·89	1·52	2·36	2 07	2·58	53·16	27·98	12·96	3·31	2·78
FeO	43·91	68·71	33·95	42·72	74·71	65·09	73·41	66·91	66·07	14·12	18·28	51·01	70·51	66·49
MnO	0·43	2·64	0·43	0·49	1·20	1·50	1·75	1 90	0·75	0·12	0·18	0·40	0·57	0·95
MgO	8·00	0·02	5·55	4·90	0 06	0·84	0·17	0·02	0·27	20·93	15·84	5·50	1·43	1·29
Cr_2O_3	28·66	0·05	46·61	38·40	0·13		0·11			11·91	37·58	20·30	5·07	0·03
Total	101·38	95·28	99·35	98·26	94·86	92·48	93·34	97·67	92·95	100·42	100·07	96·56	98·33	93·29
cr-no.	55·4		73·5	76·5						13·1	47·4	51·2	50·7	
mg-no.	34·5		27·4	23·5						81·1	69·5	24·4	5·3	

	Low-Ti										DAC
	D57	D57	D108	D108	D60	D60	D60	D130	D146	D73	D66
	E	L	E	L	E	E	L	L	L	L	L
TiO_2	1·02	27·31	0·46	10·46	1·57	9·12	22 26	16·77	25·69	24·25	9·05
Al_2O_3	21·12	2·06	38·38	2·19	19·44	9·49	6·64	4·03	1·44	1·70	0·56
FeO	40·86	66·05	21·22	79·59	26·71	37·24	66·31	65·72	69·91	67·50	80·05
MnO	0·32	0·62	0·18	0·24	0·28	0·42	2·06	0·39	0·94	0·73	0·57
MgO	5·08	2·51	15·69	0·80	10·26	7·30	0·10	3·02	0·01	0·58	0·50
Cr_2O_3	29·82		23·30		42·34	33·97		7·11			
Total	98·22	98·55	99·23	93·28	100·60	97·54	97·37	97·04	97·99	94·76	90·73
cr-no.	48·6		28·9		59·4	70·6		54·2			
mg-no.	24·5		66·3		46·7	30·6		11·3			

E, early; L, late; *cr*-no. = Cr/(Cr+Al); *mg*-no. = Mg/(Mg+Fe^{2+}).

after a slight increase from the most Mg-rich picrites to basalts (consistent with Mg-rich olivine control lines) decreases from ~8% MgO downwards. The change in slope is due to the onset of significant plagioclase and clinopyroxene fractionation. It is to be remarked that the chemical data and the petrographic features support the essential presence of plagioclase in the fractionating assemblages of the rock groups, in particular for the low-Ti group, even considering relatively Mg-rich lithotypes. This was stated also by Cox & Devey (1987) in a survey of the chemical variations in the Western Ghat basalts. SiO_2 tends to increase slightly with decreasing MgO contents. Fe_2O_{3t} is roughly constant in the basalt to basaltic andesite range. Na_2O contents continuously increase with decreasing MgO, and are almost identical in the various geochemical groups at the same MgO (Fig. 9). K_2O and P_2O_5 are significantly higher in the high-Ti groups, and generally tend to increase with decreasing MgO, albeit with scatter.

When plotted against MgO, most trace elements show clear and well-defined trends; in particular, Rb, Y, Zr, Nb and Ba increase with decreasing MgO. The remarkable differences in the contents of

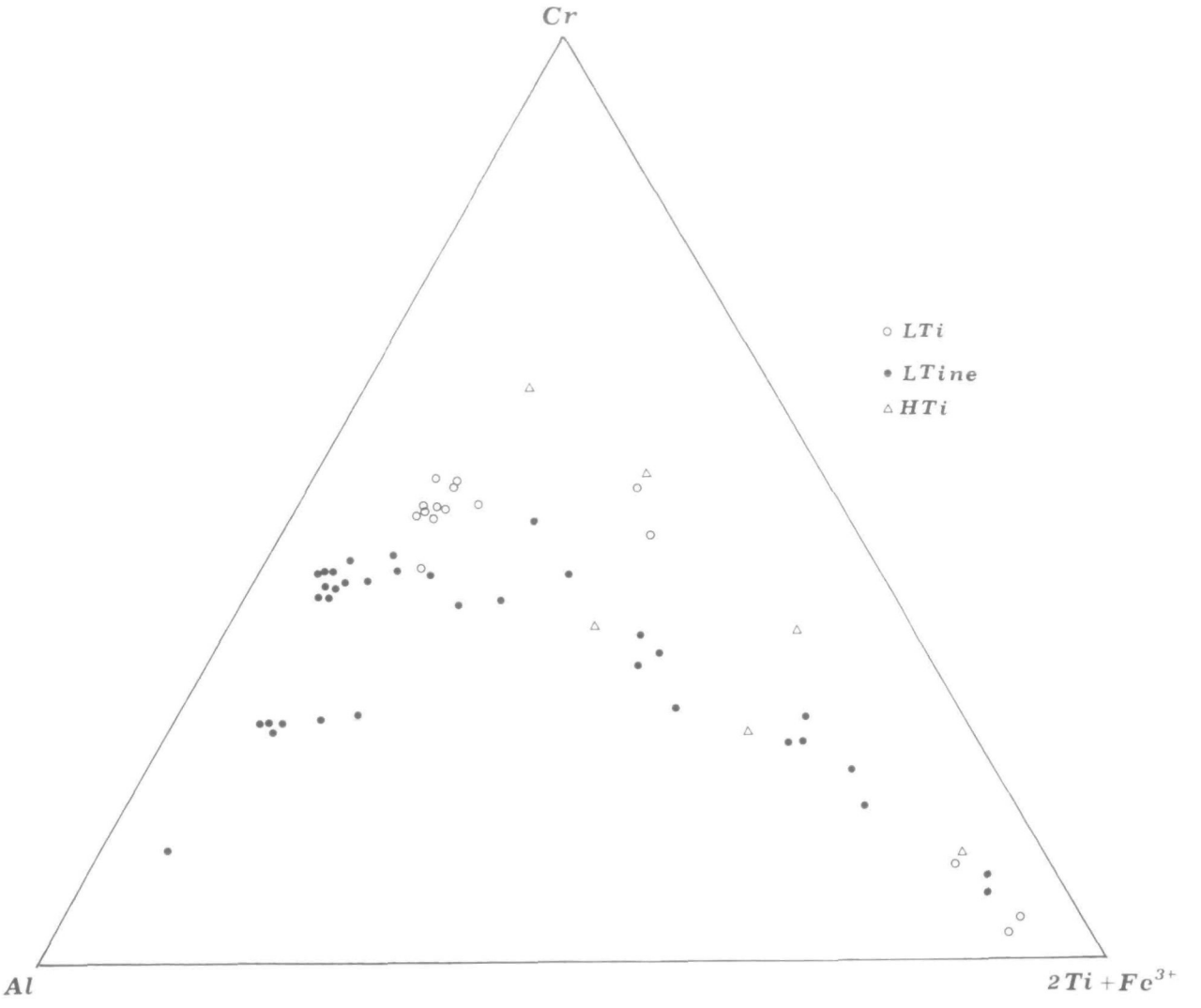

Fig. 7. Cr–Al–(2Ti + Fe^{3+}) diagram for spinels enclosed in olivine. The overall curved trend of the Cr-spinels is very clearly visible.

these elements in the picrites (and in the related basalts) are evident. It is noted, in contrast, that Y contents of low-Ti and high-Ti are completely indistinguishable, suggesting that this element did not participate in the enrichment/depletion events suffered by most other trace elements (Fig. 9).

Cr and Ni decrease markedly from picrites to basalts, decreasing from ~1000 p.p.m. and 500 p.p.m., respectively, to the low concentrations typical of differentiated rocks; the fractionation of olivine with small amounts of Cr-spinel readily explains the decrease in these two elements. V (and Zn) contents clearly increase with decreasing MgO, although the data are scattered. These trends coupled with Fe_2O_3 behaviour clearly confirm a negligible role for Fe–Ti oxide fractionation (and also sulphide for Zn) in the evolution from picrites to basaltic andesites. V (and Zn) are slightly but significantly enriched in the high-Ti rocks, at a given MgO content.

The average scandium concentrations are almost identical in the low-Ti and high-Ti picrites and are clustered around 30 p.p.m. (Fig. 9; Table 7); the concentrations in the picrite basalts tend to have a scattered, albeit slight, increase down to 8% MgO, suggesting little involvement of clinopyroxene fractionation, as is also observed in the CaO–MgO diagram. Values as high as 42–54 p.p.m., decreasing with MgO, are observed in many basalts of the low-Ti suite, whereas the data for basalts of the high-Ti suite seem to have a smoother decrease with MgO.

Dacites and rhyolites have low and decreasing TiO_2, Fe_2O_{3t}, CaO, P_2O_5, Sc and V with MgO, as well as generally higher incompatible trace element

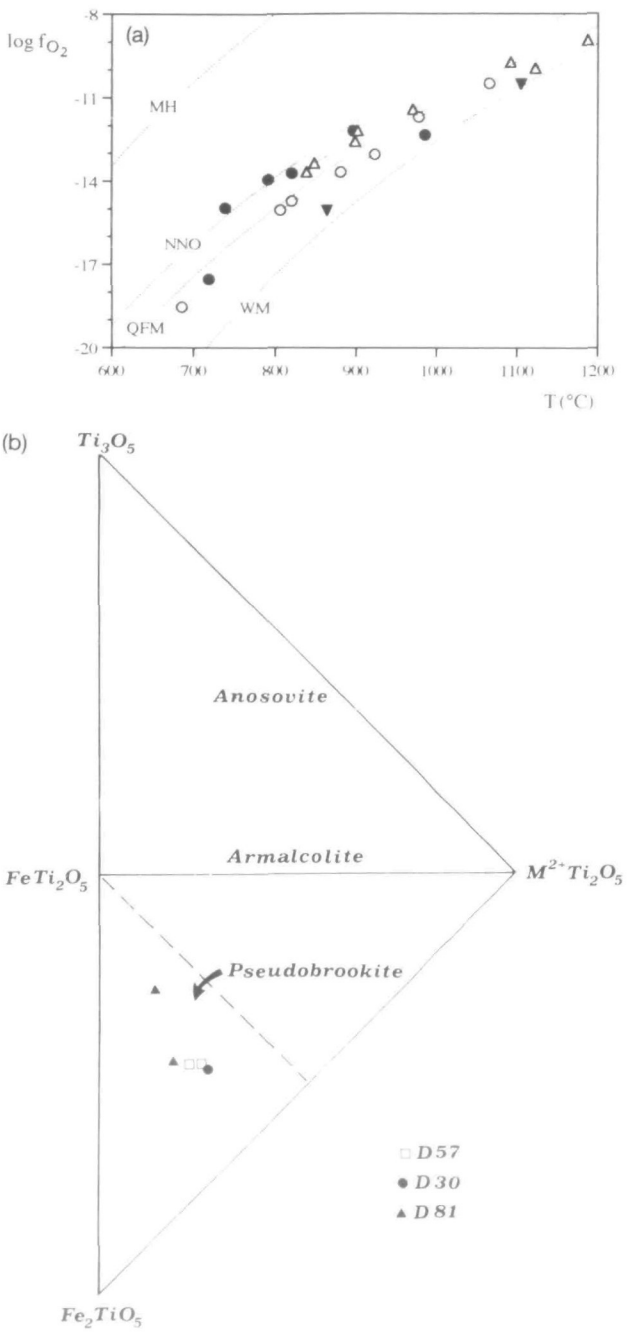

Fig. 8. (a) T–f_{O_2} diagram for coexisting Fe–Ti oxides. Open circles: low-Ti rocks; filled circles: ne-normative low-Ti rocks; filled triangles; I-Ti rocks; open triangles: high-Ti rocks. (b) Pseudobrookite compositions after Bowles (1988).

abundances (Fig. 9), when compared with basalts and basaltic andesites. The silica gap between these rocks and the most differentiated 'andesites' is noteworthy (see also Fig. 3c), and probably cannot be fully derived from crystal fractionation, unless significant amounts of low-Si phases (e.g. oxides) are involved; this, on the basis of the petrographic features, seems unlikely. Some differences between trace element contents (in particular, REE) of the various rhyolites are observed (see below).

In the Zr/Nb vs Y/Nb diagram (Fig. 10) the ranges of the major groups are well displayed. High-Ti and KT samples are characterized by low to moderate Zr/Nb (3–12) and Y/Nb (0·6–2·1) ratios, typical of incompatible element enriched basalts [E-MORB (mid-ocean ridge basalt) or WPB (within-plate basalt); see le Roex *et al.*, 1985]. I-Ti basalts plot in a straight line displaced to higher Zr/Nb values (10·4–16·6), compared with high-Ti and KT, whereas the low-Ti basalts are displaced to higher Y/Nb values (2·1–9·3), but with only slightly higher average Zr/Nb values than the I-Ti rocks (9·3–23·4). The average values of low-Ti are close to T-MORB and, to a lesser extent, to the N-MORB fields. These ratios are not much changed even after 50% fractionation of gabbroic assemblages; therefore, the different degrees of enrichment of the parental magmas of the high-Ti, KT, I-Ti and low-Ti groups are evident, as well as a moderate variability in the geochemical features within the various groups (see also below).

The REE chondrite-normalized patterns are also bimodal. The low-Ti picrite basalts are characterized by low $(La/Yb)_n$ ratios (1·7–2·9, av. 2·1), and almost flat heavy rare earth element (HREE) profiles [av. $(Gd/Yb)_n = 1·7$]; two rocks cropping out near Rajkot (D129 and D130) even show an unusual light rare earth element (LREE) depleted profile [$(La/Sm)_n = 0·8$] (Fig. 11a). However, their chondrite-normalized patterns are positively fractionated from Gd to Lu. A negative Eu anomaly is observed in some nepheline-normative low-Ti picrite basalts (D57 and D108; Eu/Eu* 0·87–0·92).

A larger LREE fractionation is observed in the high-Ti picrite basalts [$(La/Yb)_n$ 8·4–11·9, av. 10·2; Fig. 11b]; HREE fractionation is also higher than that of the low-Ti rocks [av. $(Gd/Yb)_n = 2·9$]. The K-rich basalt for which REE data are available (D207) is characterized by similar $(La/Yb)_n$ to the high-Ti rocks (10·9), but with higher REE contents, compatible with its differentiated nature (Fig. 11d); moreover, this sample does not show a negative Eu anomaly. The I-Ti rocks show an intermediate LREE enrichment [$(La/Yb)_n$ 5·2–6·2] compared with low-Ti and high-Ti analogues; negative Eu anomalies are not evident.

The evolved basalts show roughly parallel REE patterns, displaced to higher REE contents (Fig. 11e), and clear signs of an increasing role for plagioclase fractionation: Eu/Eu* decreases from 0·97 to 0·67 in the low-Ti basalt to basaltic andesite, but Eu concentrations increase. This character is observed,

Table 6: Selected analyses of ilmenites, amphiboles, phlogopites and pseudobrookites

	Ilmenites								Amphiboles			Phl
	High-Ti		I-Ti	Low-Ti					L-Ti			High-Ti
	D97	D79	D121	D57	D108	D60	D130	D105	D45	D45	D105	D79
	L	L	L	L	L	L	L	L	L	L	L	L
SiO_2	—	—	—	—	—	—	—	—	45·80	45·51	43·09	41·50
TiO_2	48·15	48·78	49·52	51·28	46·84	48·93	52·25	51·54	0·99	1·03	0·60	4·36
Al_2O_3	—	0·11	0·19	—	0·06	—	—	—	4·64	5·16	6·58	11·80
FeO	47·11	45·03	46·97	43·91	47·64	49·03	39·87	48·94	24·31	24·76	22·93	9·01
MnO	0·62	0·45	0·43	0·62	0·60	0·58	0·57	0·65	0·61	0·58	0·28	0·09
MgO	2·85	3·51	0·96	3·10	1·96	0·68	6·44	0·03	8·34	8·05	8·61	20·79
CaO	—	—	—	—	—	—	—	—	9·88	9·81	10·63	—
Na_2O	—	—	—	—	—	—	—	—	1·73	1·94	1·93	0·85
K_2O	—	—	—	—	—	—	—	—	0·66	0·64	1·08	9·67
Total	98·73	97·88	98·07	98·91	97·10	99·22	99·13	101·16	96·96	97·48	95·73	98·07
ilm	90·1	91·6	94·8	95·9	89·7	92·8	95·0	96·1				

	Pseudobrookites	
	Low-Ti	High-Ti
	D57	D81
	L	L
TiO_2	54·18	58·99
Fe_2O_3	31·52	18·30
FeO	9·51	18·20
MnO	0·62	1·04
MgO	4·00	1·77
Total	99·83	98·30
Ti	1·823	1·902
Fe^{3+}	0·531	0·295
Fe^{2+}	0·356	0·652
Mn	0·023	0·038
Mg	0·267	0·113
Total	3·000	3·000
$MO2TiO_2$	24·7	13·7
$FeO2TiO_2$	30·3	59·4
$Fe_2O_3TiO_2$	45·1	26·9

Ilmenite and pseudobrookite end-members in mol%.

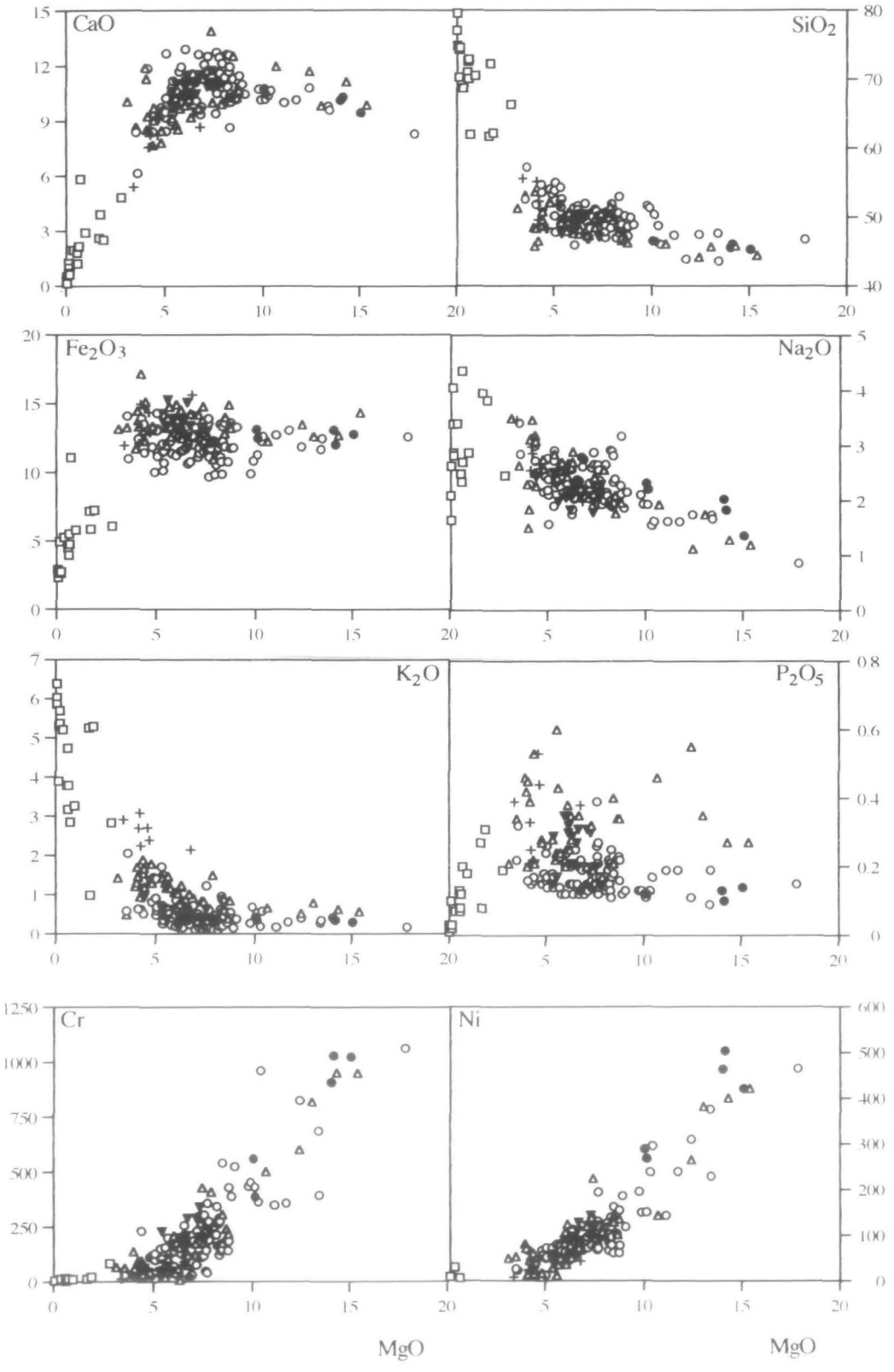
CaO
SiO2
Fe2O3
Na2O
K2O
P2O5
Cr
Ni
MgO
MgO

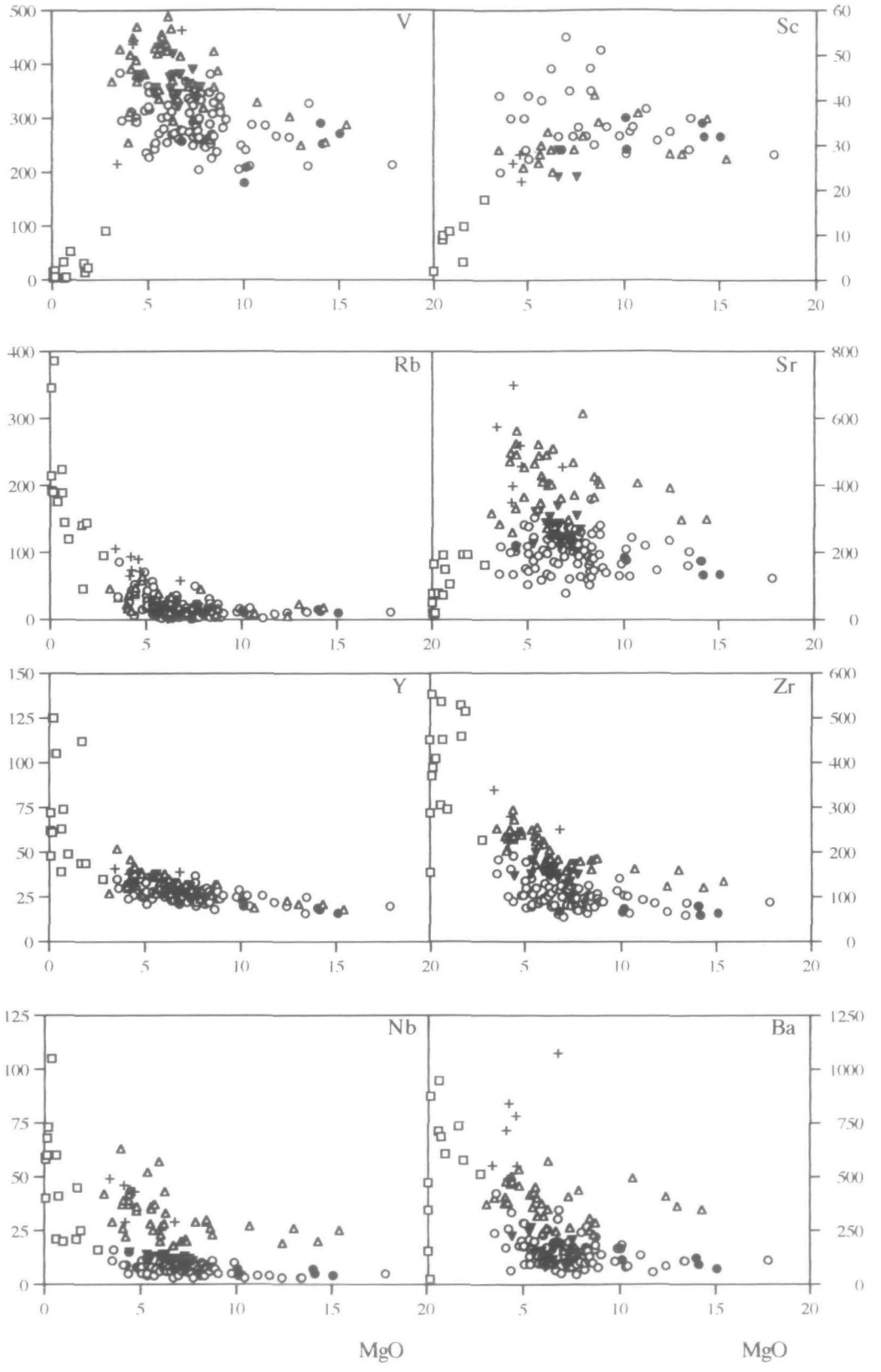

Fig. 9. Major and trace elements diagrams vs MgO content. Open circles: low-Ti rocks; filled circles: ne-normative low-Ti rocks; open triangles: high-Ti rocks; filled triangles: I-Ti rocks; crosses: KT; squares: differentiated rocks.

Table 7: Major (wt %) and trace element (p.p.m.) analyses of Gujarat samples

	High-Ti										KT				I-Ti				Low-Ti		
	81	97	44	218	168	79	128	158	165	210	224	219	213	207	121	42	152	229	60	130	129
	Pav	Pav	C Kat	Rajp	Rajp	Pav	C Kat	Pav	Rajp	Rajp	Rajp	Rajp	Rajp	Rajp	Rajkot	C Kat	C Kat	Rajp	S Kat	Rajkot	Rajkot
SiO_2	45·81	45·69	46·08	46·76	50·50	48·24	48·19	50·20	48·50	52·08	48·30	46·78	48·32	52·27	49·80	50·36	50·01	48·17	47·64	47·50	46·08
TiO_2	1·90	2·46	2·30	2 87	2·28	2·87	3·30	3·07	3·21	2·91	3·41	3·26	3·19	2·67	2·34	2·22	1·92	2·79	1·04	1·16	1·20
Al_2O_3	11·85	13·30	13·45	13·63	13·85	16·32	13·68	13·80	15·38	14·35	14·92	14·10	16·10	13·74	13·28	14·01	15·85	14·36	14·14	13·83	16·45
Fe_2O_3	12·71	12·63	12·27	14·91	12·34	12·49	14·56	13·35	13·99	13·07	14·37	15·64	12·92	13·25	12·97	12·62	11·78	15·31	11·69	11·88	12·62
MnO	0·14	0·15	0·16	0·18	0·17	0·17	0·22	0·16	0·17	0·17	0·18	0·20	0·15	0·18	0·18	0·18	0·15	0·22	0·17	0·18	0·16
MgO	14·30	13·02	10·70	8·65	7·42	6·31	6·23	5·72	5·57	4·80	4·62	6·79	4·70	4·26	7·55	6·62	6·59	5·57	13·38	12·40	10·43
CaO	11·12	9·83	11·98	10·29	10·01	9·20	10·20	9·77	8·81	7·82	8·26	8·68	9·17	8·27	10·97	11·13	10·49	11·04	9·81	10·79	10·67
Na_2O	1·28	1·75	1·93	1·96	2·42	2·89	2·61	2·55	2·57	2·75	2·68	1·99	2·59	2·86	2·08	2·29	2·31	1·99	1·74	1·75	1·63
K_2O	0·62	0·79	0·65	0·39	0·82	1·24	0·75	1·16	1·17	1·78	2·71	2·15	2·39	2·24	0·63	0·35	0·60	0·38	0·28	0·40	0·57
P_2O_5	0·27	0·35	0·46	0·34	0·19	0·28	0·25	0·23	0·60	0·28	0·53	0·38	0·44	0·25	0·20	0·20	0·27	0·17	0·09	0·11	0·17
Sc	34	28	37	35	29	24	29	30	26	25	28	—	22	26	23	29	23	—	29	33	34
V	255	364	328	387	354	294	465	455	335	383	377	462	377	444	336	382	322	432	211	264	287
Cr	952	819	500	240	427	6	58	106	18	31	50	55	62	66	191	209	170	81	687	825	961

Ni	400	381	143	101	224	50	54	81	11	8	45	43	45	45	121	109	87	48	375	309	296
Cu	75	152	92	—	—	35	205	—	—	—	—	—	—	88	150	142	—	—	67	98	108
Zn	87	98	79	127	117	99	117	131	120	122	129	142	120	123	113	111	92	132	76	77	85
Rb	18	23	9	7	18	34	11	22	32	58	90	58	72	74	14	29	10	4	12	10	17
Sr	300	297	406	414	371	510	403	429	488	365	519	455	457	699	311	287	281	324	161	236	245
Y	21	21	19	32	29	27	35	37	36	39	33	39	29	39	26	27	25	38	16	20	20
Zr	121	160	163	185	172	186	186	232	224	247	246	251	238	280	175	152	151	200	60	67	64
Nb	19·8	25·5	27·2	26	20	33	28	37	35	34	43	29	43	37	12	12	10	13	3·4	3·4	3·0
Ba	400	249	496	232	263	574	261	403	428	535	784	1076	551	841	206	168	170	146	107	85	85
Th	5	6	4	8	3	6	3	3	6	12	10	8	9	6	5	—	—	7	—	1	—
La	15·2	21·1	20·0	—	21·1	30·4	—	31·2	29·4	46·9	—	—	—	49·5	18·9	13·9	—	—	5·6	3·9	3·9
Ce	33·8	50·1	42·4	—	54·3	59·5	—	72·8	69·2	95·1	—	—	—	98·8	45·0	34·5	—	—	13·6	10·7	10·6
Nd	17·4	25·1	21·7	—	26·9	29·9	—	36·2	32·3	45·2	—	—	—	48·9	24·1	19·9	—	—	8·5	8·7	8·2
Sm	4·22	5·98	4·98	—	6·73	6·45	—	8·58	7·48	9·83	—	—	—	10·89	6·11	5·06	—	—	2·41	2·93	2 77
Eu	1·32	1·75	1·53	—	1·97	2·13	—	2·58	2·30	2·59	—	—	—	3·06	1·90	1·59	—	—	0·93	1·03	1·03
Gd	4·33	5·97	4·26	—	6·63	6·03	—	8·03	7·07	8·78	—	—	—	9·08	5·88	4·88	—	—	2·78	3·77	3·42
Dy	3·06	4·44	3·48	—	5·11	4·99	—	6·44	5·48	7·18	—	—	—	7·67	5·00	4·42	—	—	2·72	3·28	3·13
Er	1·36	2·06	1·50	—	2·50	2·27	—	3·01	2·66	3·43	—	—	—	3·45	2·34	2·01	—	—	1·45	1·66	1·80
Yb	1·09	1·70	1·23	—	2·04	2·01	—	2·48	2·13	3·00	—	—	—	3·07	2·06	1·80	—	—	1·41	1·56	1·53
Lu	0·23	0·28	0·22	—	0·36	0·34	—	0·43	0·39	0·53	—	—	—	0·47	0·35	0·27	—	—	0·25	0·30	0·29

(continued on next page)

Table 7: continued

	Low-Ti													Low-Ti ne-norm							
	120	49	45	208	107	33	47	105	102	146	211	51	73	108	57	56	58	66	16	89	21
	Rajkot	C Kat	C Kat	Rajp	S Kat	Junag	C Kat	S Kat	S Kat	S Kat	Rajp	C Kat	E Kat	S Kat	S Kat	S Kat	S Kat	DAC E Kat	Rhy Junag	Rhy Pav	Rhy Junag
SiO_2	51·67	48·89	48·61	49·93	51·03	50·10	50·03	51·95	51·07	49·94	55·01	53·33	57·26	45·27	46·05	46·47	47·06	66·32	70·52	70·05	74·57
TiO_2	0·63	1·32	1·13	0 86	1·23	1·33	0·85	1·44	1·28	1·01	1·84	0·98	1·65	0·89	0·79	1·06	1·15	0·96	0·77	0·67	0·23
Al_2O_3	14·60	16·22	14·33	15·49	15·28	15·17	14·25	15·73	13·93	16·29	14·26	16·90	14·94	14·54	14·22	15·49	17·55	13 37	12·59	13·24	13·36
Fe_2O_3	9·93	11·89	12·22	11·12	11·14	12·09	13·29	10·64	13·97	12·25	11·44	10·04	10·99	12·80	12·04	13·13	14·22	6·08	5·79	5·53	2·76
MnO	0·15	0·15	0·19	0·18	0·16	0·18	0·21	0·15	0·23	0·19	0·14	0·14	0·13	0·16	0·18	0·19	0·18	0·10	0·09	0·13	0·02
MgO	9·76	8·45	8·26	8·23	8·03	7·37	6·98	6·60	6·22	5·71	5·07	4·93	3·62	15·07	14·14	10·05	6·77	2·80	0·97	0·63	0·21
CaO	10·74	10·34	12 58	11·70	10·45	11·40	12·09	10·11	10·08	11·71	8·46	9·61	6·16	9·43	10·31	10·77	9·63	4·84	2·92	2·16	0·64
Na_2O	2·11	1·95	2·01	1·96	2·09	2·00	2·06	2·37	2·57	2·24	2·11	2·44	2·85	1·36	1·83	2·32	2·79	2·46	2·87	4·35	2·82
K_2O	0·27	0·58	0·46	0·37	0·47	0·23	0·11	0·87	0·50	0·52	1·40	1·43	2·05	0·30	0·35	0·42	0·53	2·83	3·26	3·17	5·37
P_2O_5	0·13	0·18	0·21	0·15	0·13	0·14	0·12	0·15	0·15	0·14	0·26	0·18	0·32	0·14	0·10	0·12	0·13	0·19	0·18	0·08	0·03
Sc	32	30	42	47	32	32	54	32	47	40	27	29	24	32	32	36	29	18	11	10	—
V	205	266	381	289	246	249	368	261	381	301	316	236	296	271	252	279	257	91	53	3	—
Cr	434	540	267	263	249	276	184	113	40	198	99	120	28	1025	1030	559	17	82	10	3	—
Ni	195	162	102	84	121	82	87	62	45	76	69	58	23	421	503	288	88	—	—	6	—

Cu	—	—	181	123	—	—	—	—	—	—	—	—	—	95	102	110	—	—	—	—	—
Zn	79	80	82	90	82	92	99	80	116	81	100	116	80	85	82	79	90	109	55	113	—
Rb	11	18	16	11	8	4	5	36	21	20	43	71	86	10	12	13	15	96	120	189	386
Sr	130	146	143	103	228	204	79	167	129	118	277	152	217	135	134	185	247	163	106	192	20
Y	25	26	25	24	29	25	25	30	31	27	27	26	30	16	18	23	21	35	49	63	125
Zr	114	101	78	64	97	101	55	118	101	86	178	104	183	64	60	66	68	227	296	536	389
Nb	5	7	9	5	7	6	4	6	9	4	11	7	16	3·9	4·7	7·1	7	16	20	60	73
Ba	106	129	172	98	241	195	52	194	172	136	384	203	423	72	92	166	199	513	607	947	—
Th	2	5	3	1	—	—	—	6	2	2	5	12	13	2	1	1	—	15	31	35	74
La	—	10·5	10·1	6·3	11·2	—	—	—	10·9	9·3	18·8	20·4	29·8	4·2	4·5	7·6	7·0	43·9	42·8	94·3	153·5
Ce	—	23·9	22·1	15·4	25·5	—	—	—	25·1	21·8	46·1	44·4	64·1	10·9	11·9	17·8	17·0	83·0	84·4	177·7	306·3
Nd	—	13·5	12·8	10·1	14·1	—	—	—	12·1	13·3	23·3	21·3	28·4	7·8	7·2	10·8	10·2	37·1	37·2	77·2	131·1
Sm	—	3·89	3·36	2·86	3·89	—	—	—	3·40	3·55	5·86	4·77	6·87	2·50	2·32	3·00	2·84	8·19	9·35	16·21	26·48
Eu	—	1·19	1·09	0·82	1·30	—	—	—	1·08	1·06	1·70	1·07	1·72	0·83	0·76	1·02	1·05	1·84	1·71	3·49	0·73
Gd	—	3·93	3·51	3·38	4·43	—	—	—	4·12	4·19	5·73	4·79	6·92	3·04	3·07	3·63	3·52	7·87	9·08	13·48	21·63
Dy	—	4·40	4·31	3·60	4·02	—	—	—	4·77	4·33	4·95	4·90	6·07	3·12	2·98	3·62	3·76	7·21	9·19	11·92	18·82
Er	—	2·22	2·38	2·20	2·13	—	—	—	2·65	2·54	2·41	2·67	3·13	1·75	1·58	1·96	2 05	3·74	5·28	5·48	9·06
Yb	—	2·19	2·46	2·29	1·94	—	—	—	2·99	2·51	2·10	2·66	3·02	1·67	1·54	1·80	1·87	3·74	5·33	5·51	7·96
Lu	—	0·38	0·42	0·44	0·36	—	—	—	0·51	0·44	0·37	0·45	0·51	0·30	0·27	0·34	0·35	0·63	0·89	0·83	1·29

Pav, Pavagadh; Kat, Kathiawar; Rajp, Rajpipla; Junag, Junagadh.

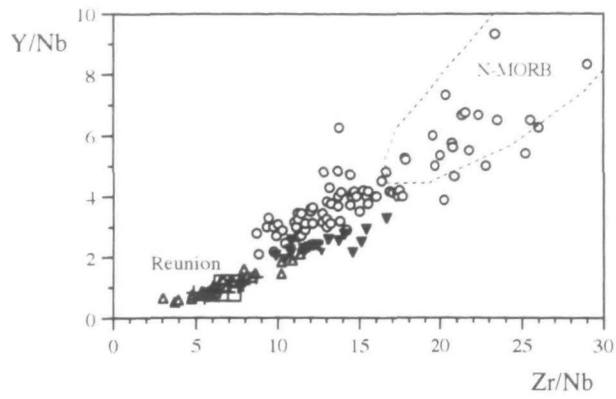

Fig. 10. Zr/Nb vs Y/Nb diagram for the basic rocks (picrites and basalts) of Gujarat. N-MORB field after le Roex *et al.* (1985) and Reunion after Fisk *et al.* (1988). +, KT, △, high-Ti; ▼, I-Ti; ○, low-Ti.

for example, in the very low-Ti basaltic andesite to dacite CFB sequence of the Ferrar group, Antarctica (Brotzu *et al.*, 1992), and confirms that Eu still has a $D<1$ in rocks dominated by fractionation of plagioclase-rich assemblages. The differentiated rocks (dacites and rhyolites) show relatively high REE concentrations and patterns with variable LREE fractionation. These differentiated samples have different characters when found associated with different magma groups (Fig. 11f). In particular, the D16 rhyolite, cropping out in central–eastern Kathiawar and associated with low-Ti rocks, and the D89 pitchstone, cropping out at the top of the Pavagadh sequence made up only of high-Ti rocks (Fig. 1b), are interesting in this respect. The LREE fractionation is higher in the Pavagadh rhyolite [$(La/Yb)_n$ of D89 is 11·5 vs 5·4 for D16], and the Eu negative anomalies are more pronounced in the Kathiawar rhyolite (Eu/Eu* 0·56 against 0·7). The higher Nb, Zr, Rb, Ba and REE contents, and lower La/Nb ratio of the Pavagadh sample (1·6 vs 2·2 for D16; see Table 7) rule out clear genetic links between these two rhyolites.

Mantle-normalized patterns for selected rocks and averages of the different groups are given in Fig. 12. Some features can be emphasized: (1) the broad ocean-island basalt (OIB)-like pattern for the high-Ti picrites, with overall high trace element abundances and a slight negative K spike (Fig. 12a); (2) a less enriched pattern for the low-Ti picrites, with average values close to 10 times mantle, and showing high normalized abundance for Rb, Ba, Th and K with respect to Nb, LREE and Sr, and with a weak negative spike for Ti and Nb, differently from N-MORB (Fig. 12b, d); (3) the higher normalized abundance for LILE and LREE in the KT rocks, when compared with average high-Ti of the same evolution degree (Fig. 12c). The patterns of I-Ti rocks are characterized by lower enrichment in most incompatible elements compared with the high-Ti picrites, even considering that no primitive rocks are available for this magma group. The I-Ti rocks also show slight Nb, Sr and P negative anomalies, but no negative Ti spikes (Fig. 12c). When compared with the average data on Western Ghats basalts (Lightfoot *et al.*, 1990), the HFSE abundance of the Low-Ti picrites is comparable only with that of the Bushe formation (Fig. 12b). However, the LREE enrichment in the low-Ti rocks is, on the average, lower than that in the average Bushe basalt (Lightfoot *et al.*, 1990), which is characterized, however, by a higher degree of differentiation (and probably contamination).

GEOCHEMICAL CHARACTERS OF THE GUJARAT PICRITES AND IMPLICATIONS FOR THEIR MANTLE SOURCES

The significant number of primitive picrites found in the Gujarat area, and the unusual depleted patterns of some of them, relative to the analyses already published (e.g. Krishnamurthy & Cox, 1977) clearly warrant further investigation. We normalized the rocks with >8·7 wt % MgO (for high-Ti >10 wt %) to 15 wt % MgO by fractional addition of liquidus olivine (according to $K_d = 0{\cdot}33$; Roeder & Emslie, 1970). With this MgO content, the rocks possess *mg*-number (with $Fe_2O_3/FeO = 0{\cdot}15$) varying from 0·71 to 0·76, well within the values of primary magmas of Frey *et al.* (1978), and capable of equilibrating with mantle olivine of Fo_{88-90} composition. The picrite analyses of Krishnamurthy & Cox (1977), and two Mg-rich Bushe basalts (L. Melluso, unpublished data, 1993) were added to the data set; also, these rocks do not show evidence for fractionation other than of olivine (± chromite). The picrites of Beane & Hooper (1988) were not added to the data set, as those researchers gave evidence of olivine and clinopyroxene enrichment. The trace elements incompatible in olivine were diluted accordingly, and no correction was performed for Cr and Ni. A maximum of ~19% olivine was added to the least primitive basalts to reach the utilized MgO (in some cases olivine was subtracted) (Table 8). A similar MgO window (14–16%) was used by Ellam & Cox (1989, 1991) in their study of the Letaba picrites of Karoo, by Sweeney *et al.* (1991) in their survey of the Karoo–Antarctica flood basalts and by Scarrow & Cox (1995) for the Skye basic lavas (15%). A value of 16% MgO was used by Krishnamurthy & Cox

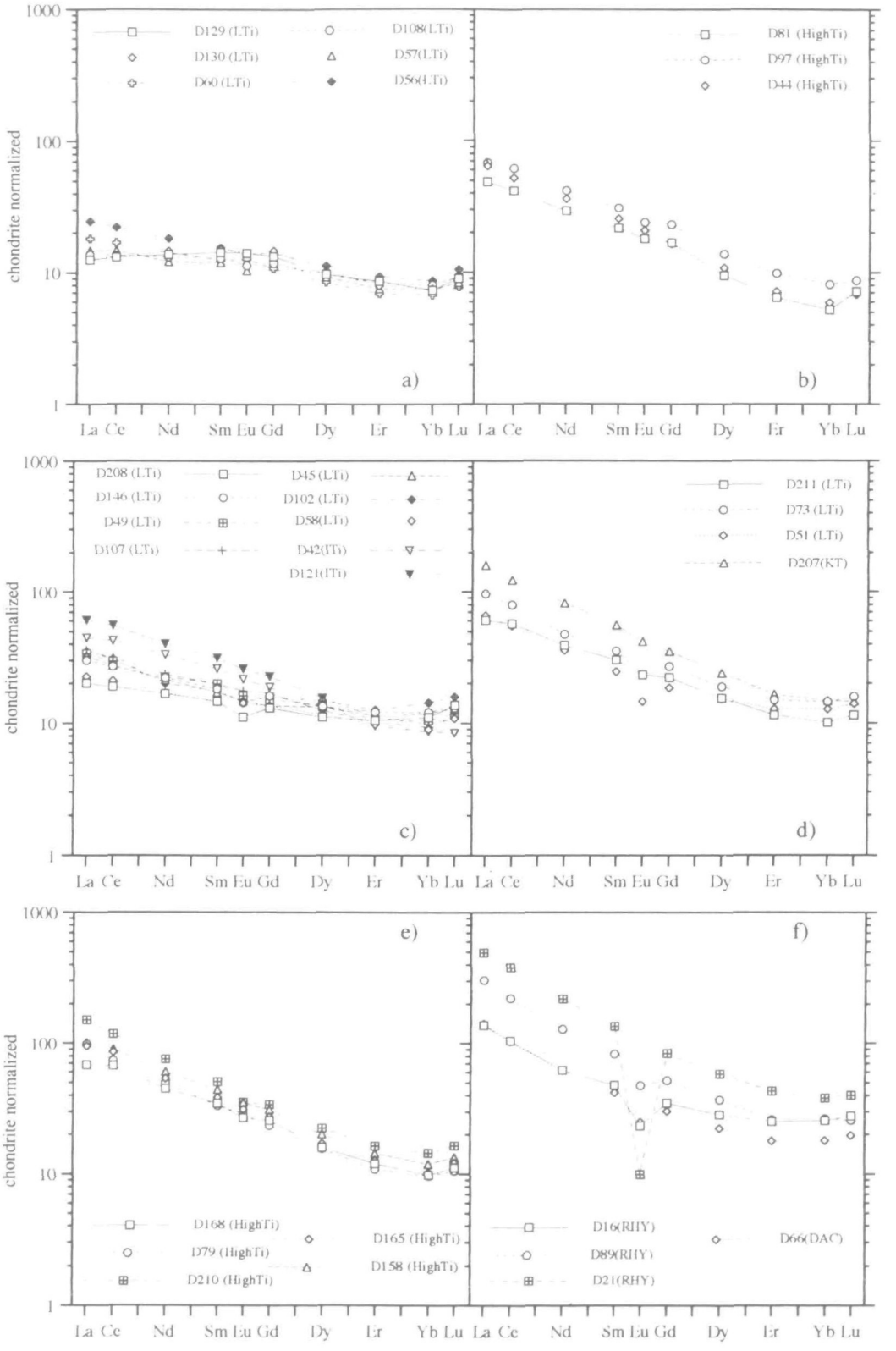

Fig. 11. REE-chondrite normalized diagrams for selected Gujarat samples. Normalization values after Boynton (1984). (a) Low-Ti picrites; (b) high-Ti picrites; (c) I-Ti, low-Ti basalts; (d) low-Ti basaltic andesites, 'andesite' and KT basaltic andesite; (e) high-Ti basalts; (f) differentiated rocks (dacite and rhyolites).

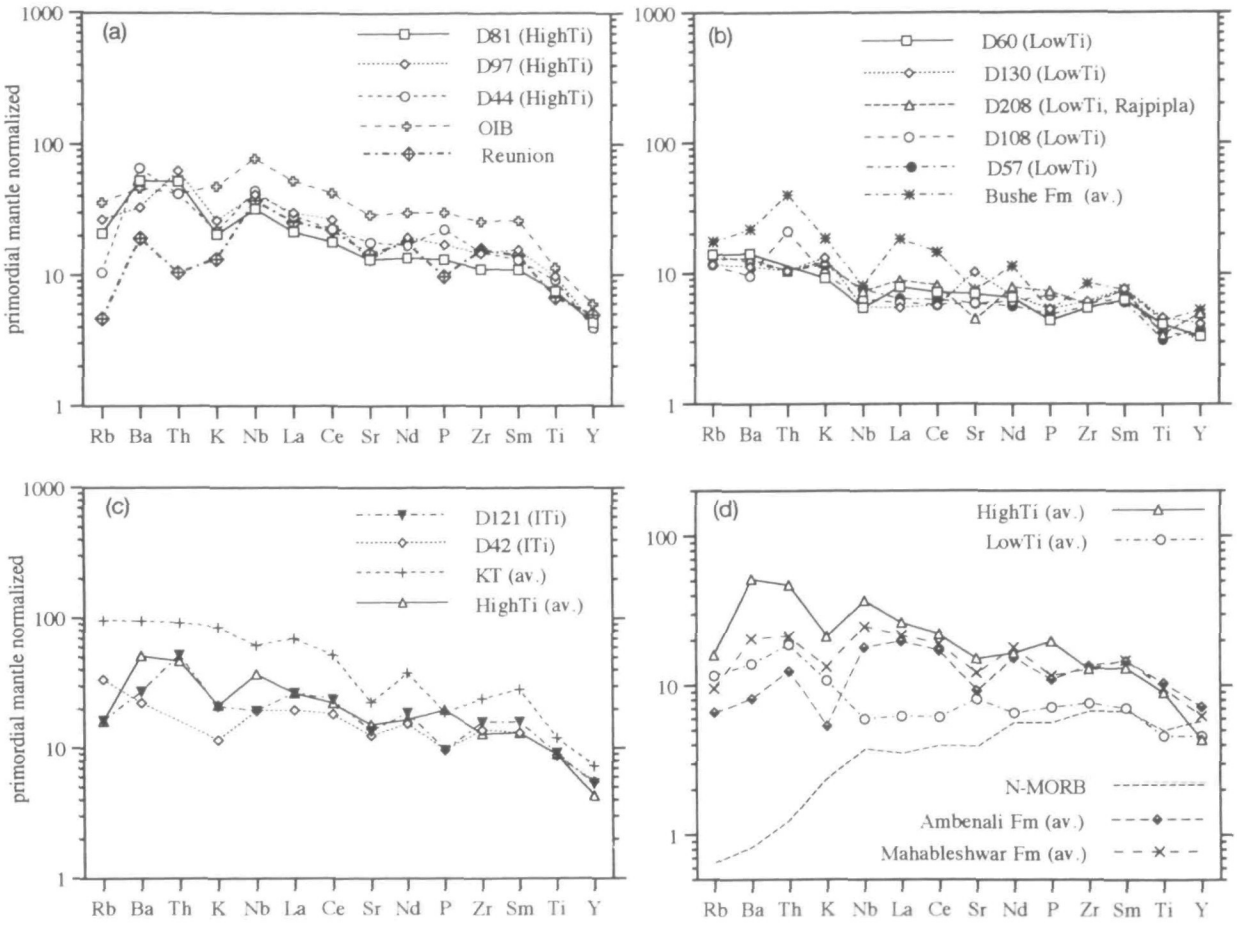

Fig. 12. Wood's primordial mantle-normalized patterns (Wood, 1979) for selected samples, averages of the various groups, Western Ghat basalts and oceanic basalts (after Fisk *et al.*, 1988; Sun & McDonough, 1989; Lightfoot *et al.*, 1990).

(1977) for the most primitive liquids of the Dhandhuka borehole, whereas a higher value (~18% MgO) was used by Holm *et al.* (1993) for the West Greenland picrites.

Despite the uniform MgO, the normalized data show a significant range for most major and trace elements: for instance, SiO_2 ranges from 45·1 to 49·8%, with substantially identical ranges for both low-Ti and high-Ti picrites (Table 8; Fig. 13). Both groups vary from hy- to ne-normative. The variation in the Si saturation is found to be mainly dependent on the SiO_2 content of the rocks, and very subordinately on the different K_2O (Na_2O is nearly constant). Fe_2O_{3t} ranges from 11·4 to 14·5%. At a given SiO_2 content, the high-Ti picrites have more CaO (11·1 ± 0·9 wt % against 9·2 ± 0·4 wt %), TiO_2 (2·04 ± 0·2 wt % against 1·00 ± 0·2 wt %), K_2O (0·73 ± 0·14 wt % against 0·32 ± 0·12 wt %), Ba (331 ± 93 p.p.m. against 110 ± 33 p.p.m.), Zr (136 ± 14 p.p.m. against 77 ± 17 p.p.m.), six times as much Nb (30 ± 7 p.p.m. against 5 ± 2 p.p.m.), higher LREE, Zr/Y (6·5 ± 1·1 against 3·8 ± 0·5), Ti/V (47 ± 5 against 27 ± 5) and less Al_2O_3 (10·4 ± 1·2 wt % against 12·8 ± 0·9 wt %), with lower Zr/Nb (4·7 ± 1·1 against 17 ± 5) and Ba/Nb (11·7 ± 4·4 against 24 ± 7) than the low-Ti picrites.

The average CaO/Al_2O_3 (0·72 ± 0·05), CaO/TiO_2 (9·6 ± 2·3) and Al_2O_3/TiO_2 (13·5 ± 3·3) ratios of the low-Ti picrites are different from the chondritic values (0·81, 15·9 and 19·7, respectively). The slightly lower than chondritic CaO/Al_2O_3 values, together with the low abundance of incompatible elements, suggest the partial melting of clinopyroxene- and Ti-poor mantle sources. On the other hand, the significantly higher average CaO/Al_2O_3 (1·1 ± 0·2) and lower CaO/TiO_2 (5·5 ± 0·7), Al_2O_3/TiO_2 (5·1 ± 0·6) of the high-Ti picrites (Fig. 14a) suggest that different sources were involved; in particular, the source of the high-Ti magmas was significantly enriched in clinopyroxene and TiO_2.

CaO/Al_2O_3 and, to a lesser extent, CaO/TiO_2 in the high-Ti group decrease with SiO_2. If the low

Table 8: Normalized major and trace elements for the picrite data set, including data of Krishnamurthy & Cox (1977; labelled KC) and two samples from Bushe Fm (collected along the Pune–Bombay road)

	44	D10	97	81	D12	D11	D6	W1	129	108	101	56	30	8	57	10	130	155	140	60	147	106	63	141	117	120	BU4	BU2
	HTi	KC	HTi	HTi	KC	KC	KC	KC	LTi	LTi	LTi	LTi	LTi	LTi	LTi	LTi	LTi	LTi	LTi	LTi	LTi	LTi	LTi	LTi	LTi	LTi	Bushe	Bushe
SiO_2	45·21	45 22	45·36	45·69	46 65	47 10	47·64	48·69	45 17	45·28	45·41	45·44	45·44	45·57	45·89	46·57	46·94	46·99	47·26	47·27	47·39	47·49	48·11	48·80	49·52	49·80	47·13	50·00
TiO_2	2·00	2·20	2·32	1·86	1·88	2 04	1·95	2·06	1 04	0·89	1·18	0·91	0·83	1·08	0·77	1·33	1·07	1·33	0·95	0·99	1·01	0·97	1·03	1·12	0·99	0·53	0·95	1·02
Al_2O_3	11·72	10·56	12 52	11·60	9·43	9·52	9 28	9·11	14·22	14·57	12·80	13·24	14·23	11·73	13·85	13·50	12·79	12·16	11·88	13·45	13·44	12 98	12·23	11·98	11·70	12·38	12·30	11·26
Fe_2O_3	12·74	12·84	12 63	12·71	11·84	12 01	11 70	11·39	13·06	12·80	13·09	13·53	12·97	14·47	12 05	12 72	11·93	12·51	13·74	11·73	12·60	12·77	12·51	11·96	11·59	10·84	12·51	10·97
MnO	0·17	0·17	0·15	0·14	0·14	0·17	0·18	0·20	0·17	0·16	0·19	0·19	0·18	0·20	0·18	0·13	0·18	0·17	0·19	0·17	0·15	0·18	0·19	0·18	0·17	0·16	0·19	0·16
MgO	15·00	15·00	15·00	15·00	15·00	15·00	15·00	15·00	15·00	15·00	15·00	15·00	15·00	15·00	15·00	15·00	15·00	15·00	15·00	15·00	15·00	15·00	15·00	15·00	15·00	15·00	15·00	15·00
CaO	10 48	10·86	9·28	10·89	12·37	11 39	11·84	11·81	9·27	9·45	9·84	9·26	9·05	8·85	10·05	8·95	10·00	9·51	8·77	9·35	9·07	9·00	9·17	8·78	8·70	9·16	9·46	9·24
Na_2O	1·68	1·86	1·65	1·25	1·54	1 79	1·37	0·92	1·41	1·36	1·97	1·98	1·90	2·57	1·78	1·45	1·62	1·75	1·80	1·66	0·94	1 34	1·55	1·65	1·65	1·79	1·73	1·71
K_2O	0·57	0·99	0·74	0·61	0·86	0·69	0·77	0·57	0·49	0·30	0·41	0·36	0·30	0·32	0·34	0·15	0·37	0·45	0·32	0·27	0·19	0·16	0·12	0·45	0·58	0·23	0·57	0·47
P_2O_5	0·40	0·31	0·33	0·26	0·29	0·30	0·26	0·24	0·15	0·14	0·13	0·10	0·10	0·18	0·10	0·17	0·10	0·13	0·11	0·09	0·16	0·11	0·10	0·09	0·11	0·11	0·16	0·17

Table 8: continued

	44	D10	97	81	D12	D11	D6	W1	129	108	101	56	30	8	57	10	130	155	140	60	147	106	63	141	117	120	BU4	BU2
	HTi	KC	HTi	HTi	KC	KC	KC	KC	LTi	LTi	LTi	LTi	LTi	LTi	LTi	LTi	LTi	LTi	LTi	LTi	LTi	LTi	LTi	LTi	LTi	LTi	Bushe	Bushe
Sc	32		26	35					29	32	34	31	25	41	31	34	31		28	28	31	28		24		27	35	32
V	286	285	234	250	259	237	260	272	248	272	281	153	178	275	245	255	244	255	247	201	234	182	233	206	212	174	251	243
Zn	69	66	92	85	71	88	74	116	73	85	96	67	70	88	80	92	71	68	76	72	91	67	70	68	61	67	81	71
Rb	8	29	22	18	25	26	22	12	15	10	15	11	9	4	12	2	9	19	7	11	12	7	2	9	14	9	13	16
Sr	354	348	280	294	321	269	258	131	212	136	171	158	151	205	131	197	218	232	115	153	137	111	128	180	140	110	157	129
Y	17	24	20	21	21	20	22	26	17	16	18	20	17	23	18	23	18	20	22	15	22	22	20	21	25	21	23	22
Zr	142	161	150	118	122	134	127	130	55	64	78	56	64	78	59	84	62	88	74	57	96	88	74	89	121	97	69	78
Nb	24	44	24	19	35	32	28	35	3	4	6	6	4	6	5	3	3	9	4	3	5	3	6	4	9	4	4	6
Ba	432	475	343	340	344	279	288	150	73	72	117	142	97	179	90	121	79	150	115	102	122	68	65	157	140	90	206	105
Th	3		6	5						2	2	1		1	1	1	1	2	3		2		1	3	8	2		
La	17·4		19·9	14·8					3·3	4·2		6·5			4 4		3·6			5 3								
Ce	36·9		47·1	33·0					9·1	10·9		15 2			11 6		9·9			12·9								
T	1467	1467	1466	1463	1456	1452	1448	1440	1468	1467	1466	1465	1465	1464	1462	1456	1453	1453	1451	1451	1450	1449	1444	1439	1434	1432	1452	1430
P(A92)	27	27	27	25	22	21	19	17	27	27	26	26	26	26	25	22	21	21	20	20	20	20	18	16	15	14	21	14
P(HK66)	28	28	28	26	23	21	19	15	29	28	28	27	27	27	26	23	22	21	20	20	20	19	17	14	11	10	21	9
Z	87	87	85	82	72	68	63	55	87	86	85	84	84	83	79	73	69	69	66	66	65	64	60	55	50	48	68	47

T(°C) = 2000 MgO/(MgO+SiO_2)+969 (Albarède, 1992).
P(A92) (kbar) = exp(0·00252T − 0·12SiO_2+5·027) (Albarède, 1992).
P(HK66) (kbar) = 206·7 − 3·945SiO_2 (Hirose & Kushiro, 1993).
Z (km) = 3·02P+5 (Scarrow & Cox, 1995).
HTi, high-Ti; LTi, low-Ti.

JOURNAL OF PETROLOGY VOLUME 36 NUMBER 5 OCTOBER 1995

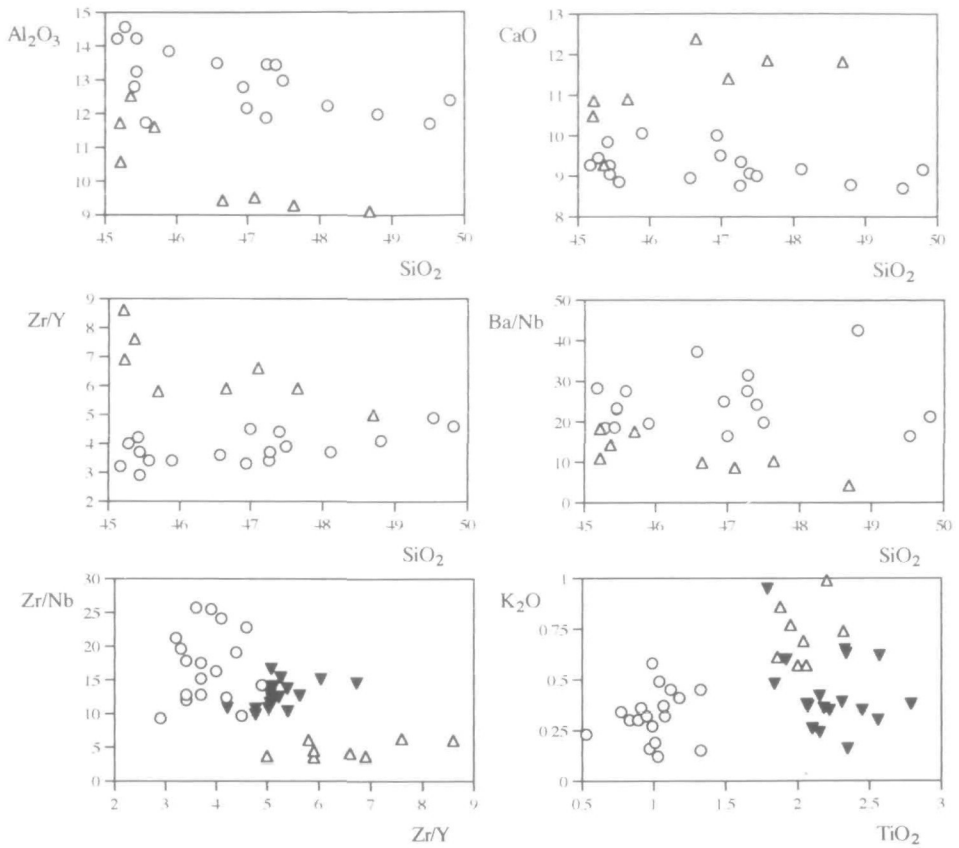

Fig. 13. Selected plots with the data on normalized picrites of Gujarat. Circles, low-Ti picrites; triangles, high-Ti picrites. I-Ti basalts (reversed, filled triangles) are shown for comparison.

SiO_2 content is linked to pressure increase (see below) it may be argued that: (1) the mantle source tends to increase in cpx with decreasing depth and/or, (2) Al_2O_3 may be more compatible owing to residual Al-bearing phases (e.g. spinel or orthopyroxene).

The Ti/Zr of low-Ti picrites shows large variation (33–113; Table 8), suggesting some decoupling of the behaviour of the two elements. Also, Ba/Nb and Zr/Nb are variable (Fig. 13). We can therefore deduce that the low-Ti mantle sources, similar with respect to the major elements, show some slight variations in the incompatible element contents and ratios which are not likely to be a function of different degrees of partial melting or pressure changes. The two Bushe picrites show relatively high SiO_2 contents, and give evidence of substantially similar mantle sources to the low-Ti picrites, at least for the major elements.

It is also interesting to note that no correlation between Ba/Nb, K_2O and SiO_2 is observed; therefore, crustal contamination processes acting on the low-Ti picrites seem very unlikely. On the other hand, the Ba/Nb ratios of the low-Ti picrites are much higher than average N-MORB values (4·3; Sun & McDonough, 1989), and testify to a clear LILE/HFSE fractionation.

The most important suggestion from these data is the complete decoupling of the mantle sources, which cannot be the result of different degrees of partial melting, starting from a homogeneous lherzolite. The geochemical characteristics of the low-Ti and high-Ti picrites give some evidence that the I-Ti basalts (Fig. 13) and the K-rich tholeiites do not have analogues in the most Mg-rich rocks, and that no clear mantle source relationships for these latter groups are available at present.

Pressure and temperature estimates

A very marked negative correlation between Fe_2O_{3t} and SiO_2 is observed in the normalized data set (Fig. 14b). This correlation is similar to that observed in many oceanic and continental primitive rocks (Klein & Langmuir, 1987; Scarrow & Cox, 1995) and in recent experimental results at variable pressures (10–30 kbar) and temperatures (1250–1525°C) on anhydrous peridotites (Hirose & Kushiro, 1993). In particular, the SiO_2–Fe_2O_{3t}

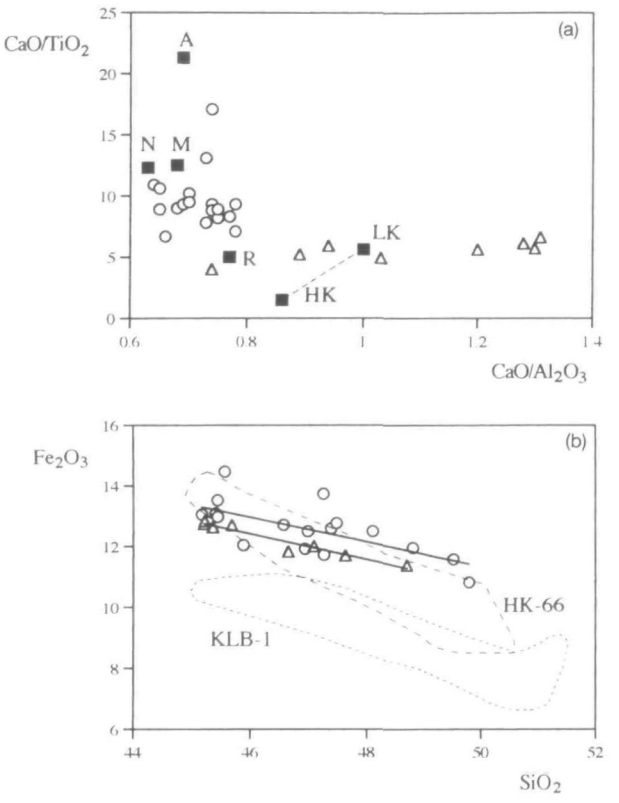

Fig. 14. Diagrams of CaO/Al_2O_3 vs CaO/TiO_2 (a) and SiO_2 vs Fe_2O_3t (b) with data on the normalized picrites of Gujarat. Circles, low-Ti picrites; triangles, high-Ti picrites; A, Ferrar inferred parental magma; N, M, Nuanetsi and Malawi low-Ti picrites; R, Reunion parental magma; LK, HK, asthenospheric and lamproitic end-members of Karoo [data from Fisk *et al.* (1988), Ellam & Cox (1991) and Sweeney *et al.* (1991)]. The fields labelled HK-66 and KLB-1 are the results of melting experiments on these two peridotites obtained by Hirose & Kushiro (1993). The lines are the best fits of the low-Ti and high-Ti data.

trend of the low-Ti and high-Ti picrites is significantly similar to the experimental data on the HK-66 Fe-rich (and opx-rich) peridotite. This suggests the involvement of mantle sources significantly Fe rich compared with those of other tectonic settings. There is, however, a slightly different Fe–Si slope with respect to the HK-66 trend (Fig. 14b); this may also imply that the Gujarat mantle sources were slightly changing in composition with depth. The variations in these two elements may be the result of the equilibration of basaltic melts with peridotite at variable pressures, and, in particular, the more SiO_2-poor (and Fe_2O_3-rich) melts are capable of equilibrating with mantle peridotite at higher pressures than high-SiO_2 melts (Yoder & Tilley, 1962; Klein & Langmuir, 1987; McKenzie & Bickle, 1988; Hirose & Kushiro, 1993).

Attempts to give pressure and temperature estimates according to experimental data were made. Utilizing the SiO_2–P regression data of HK-66 from Hirose & Kushiro (1993), and thus assuming dry melting, the pressure range for low-Ti picrites varies from 29 to 11 kbar, and for the high-Ti picrites from 29 to 15 kbar. Substantially similar results (28–15 kbar for low-Ti and 28–17 kbar for high-Ti picrites) were obtained with the algorithm of Albarède (1992). These pressure estimates imply that the Gujarat picrites may have formed over a depth range of ~40 km (87–48 km).

Temperature estimates were subjected to comparatively more uncertainty. The simple algorithm of Albarède (1992) was used for the calculations, and gave temperature ranges from 1468 to 1430°C, but the values are probably subject to the MgO imposed on the normalized samples, at least for the lowest pressures. These P–T estimates are plotted in Fig. 15. Some of the samples plot very close to or at the anydrous peridotite solidus of McKenzie & Bickle (1988); this implies that a potential temperature of ~1430°C may have been reached by an adiabatically upwelling mantle in the Gujarat area. It is remarked that the bulk of the data do not fit an adiabatically melting regime, as the average gradient for the observed trend ($\Delta T/\Delta P$) is 2·7°C/kbar, distinctly lower than the value of ~7°C/kbar (Kostopoulos & James, 1992) of the solid + melt adiabatic gradient. As a consequence, the calculated P–T data cross-cut other adiabatic gradients of higher potential temperatures (Fig. 15).

It is noted that the obtained mantle potential temperature of the samples closer to the solidus is distinctly higher than that of asthenospheric MORB-

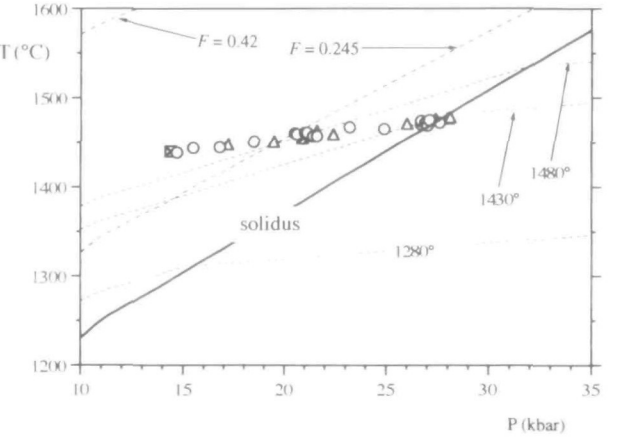

Fig. 15. P–T diagram for the Gujarat (and some Bushe Fm) picrites. Circles, low-Ti picrites; triangles, high-Ti picrites; squares with crosses, Bushe. The dashed lines labelled 0·42 and 0·245 are the F values for cpx-out from Kostopoulos & James (1991) and McKenzie & Bickle (1988), respectively. The adiabatic upwelling paths (subsolidus and suprasolidus) for potential temperatures of 1280°, 1430° and 1480°C are also shown.

mantle (~1280°C, McKenzie & Bickle, 1988), and this seems to be a reliable argument in favour of plume-driven magmatic activity in this area of the Deccan Traps.

There is an apparent absence of garnet in the mantle source of the Gujarat picrites. Assuming that the rocks with lower SiO_2 come from the greatest depths (see above), the data for Al_2O_3, Sc and Y give very little or no indication of garnet control; Al_2O_3, strikingly, has a clear negative correlation with SiO_2. Also, Zr/Y ratios do not show negative correlation with SiO_2, as expected from residual garnet control low in a melting column (Fig. 13).

The weak HREE fractionation and the relatively high Sc concentrations seem also to suggest that the primary magmas suffered the final equilibration in a garnet-free mantle. Modelling of the Sc contents in reasonable mantle sources was performed (Table 9). This element was chosen for its very different partitioning between spinel and garnet, and its relative insensitivity to trace element enrichment processes, which doubtless affected, for instance, REE abundance and fractionation. The results give evidence that small amounts of garnet left behind in the source could not justify the high Sc contents in picrites, unless a source enriched in Sc [considerably more than the 17 p.p.m. value of Jagoutz *et al.* (1979), which is probably an upper limit for undepleted mantle] was involved. On the other hand, residual sources with (or without) spinel more closely approximate Sc partitioning.

The chemical data are also in broad agreement with the experimental results of Eggins (1992) on primitive Hawaiian tholeiites. Eggins showed that garnet was present at or near the liquidus of the tholeiites at pressures of not less than 35 kbar. This value is substantially higher than the highest pressure estimate for the Gujarat (~29 kbar).

As stated above, Na_2O, HREE, Sc and Y concentrations are broadly similar for both high-Ti and low-Ti primitive rocks. These characters are at variance with the strong differences in many major and most incompatible trace elements, and seem also to indicate substantially similar degrees of partial melting, along with SiO_2 contents.

A relatively shallow source for the Deccan Trap magmas was proposed by Sen (1988), mainly on the basis of high-pressure phase diagrams.

EVOLUTION PROCESSES

The notable variations of the chemical composition of the Gujarat rocks contrast with the relatively monotonous basaltic chemistry of the rocks of the Western Ghats. Strongly differentiated basaltic andesites, 'andesite' and rhyolitic rocks, found within the sequence (or, as at Pavagadh, at the top of the basalt sequence) are not uncommon lithotypes. In the Gujarat area, apart from the various basalt groups, the tectonic regime allowed the possibility of both rapid ascent to the surface (and so allowed the presence of picrite basalts in the sample recording)

Table 9: Modelling of Sc behaviour in Gujarat picrites

			Residual sources (10% melting)		
	K_d Sc (Frey *et al.*, 1978)		gt-per	sp-per	
zol	0·27	ol	65	62	
opx	0·53	opx	28	27	
cpx	2	cpx	3	9	
sp	0·05	sp		1	
gt	6·5	gt	4		
	C_l (p.p.m.)	C_o (p.p.m.)		mantle Sc	
		sp	gt	17	Jagoutz *et al.* (1979)
High-Ti	28	15·2	19·0	14·9	Hofmann (1988)
Low-Ti	29	15·7	19·7	12	McDonough (1991)

Mode of residues after Kostopoulos, 1991 (sp-per) and McDonough, 1991 (gt-per)
$C_o = C_l \times [D_{res} + F(1 - D_{res})]$.
D_{res}, bulk partition coefficient of the residues.

and local prolonged residence of the magmas in the crust, with production of small amounts of tholeiitic differentiates and, probably with superimposed processes, rhyolites.

There is clear evidence that at least some of the low-Ti and high-Ti picrite basalts may be parental magmas to the more evolved lithotypes; this is slightly different from the case observed in the Karoo, where many picrites of the Letaba Fm are too incompatible element rich to be parental magmas of the overlying Sabie River Fm (Sweeney *et al.*, 1994). The overall higher trace element contents in basalts and basaltic andesites of Gujarat support this argument, and the substantially identical trace element ratios of the picrites and basalts give additional significant evidence.

In the pseudo-ternary phase diagram Ol–Cpx–Qz (Grove *et al.*, 1982; Fig. 16) most basalts of the various groups plot close to or at the ol + pl + cpx cotectic at 1 atm, as expected from low-pressure magmatic evolution. However, a large proportion of the low-Ti rocks are slightly displaced from this cotectic towards the olivine apex, and confirm that in this group pyroxene co-precipitates with olivine and plagioclase only at a late stage. The nepheline-normative low-Ti rocks plot at or near the ol–cpx join, closer to the olivine apex, in contrast to most low-Ti basalts. The I-Ti rocks plot in a narrow field close to the 1-atm cotectic, whereas high-Ti and KT rocks are scattered at or near the cotectic. The normalized-picrite field is also plotted, and shows the wide range of primary compositions.

Temperature estimates were used to constrain roughly the onset of the main crystallizing phases. Using the algorithm proposed by Eggins (1993), based on the MgO content of the rocks, the liquidus (= olivine-in) temperature of these picrites at 1 atm is calculated as ~1320°C. This value is similar to that experimentally obtained on High-Ti picrites at 15 wt% MgO by Krishnamurthy & Cox (1977) (~1350°C). The onset of plagioclase crystallization for both high-Ti and low-Ti (at ~1200°C; see mineral chemistry) is at ~8·3% MgO, in good agreement with the kink in the CaO–MgO trend. On the other hand, the maximum temperature obtained with two pyroxenes (and with only

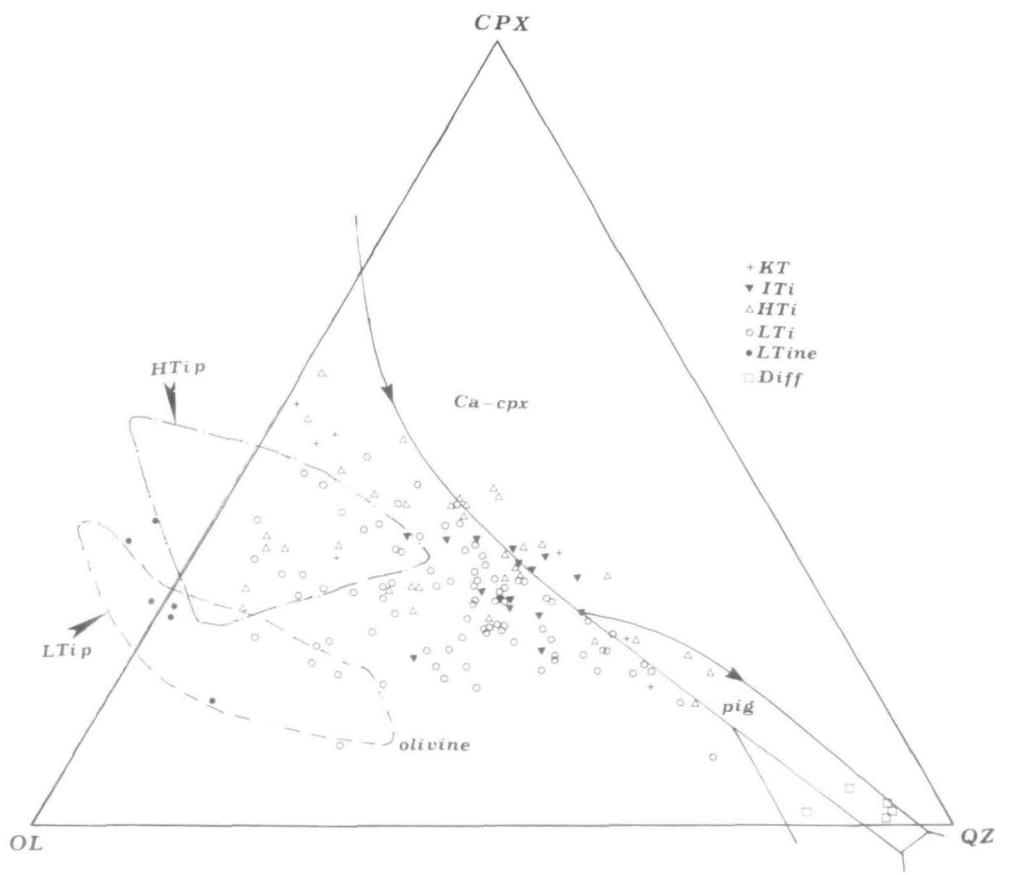

Fig. 16. Ol–Cpx–Qz pseudoternary phase diagram (after Grove *et al.*, 1982) for the basaltic rocks of Gujarat. Some acid rocks and the ranges of the normalized picrites are plotted for comparison.

pigeonite) corresponds to an MgO of ~6·1%. It is important to note that this is a significant value only for some low-Ti rocks, as pigeonite is not widespread; however, it is compatible also with the decrease from the highest Sc contents of mildly differentiated low-Ti basalts (Fig. 9). On the other hand, diopsidic clinopyroxene may be crystallized at significantly higher temperatures in the high-Ti basalts; as observed in some thin sections, these temperatures may be similar to or even very slightly higher than those of plagioclase [see also the experimental data of Krishnamurthy & Cox (1977)].

The clear differences in CaO and Al_2O_3 contents between low-Ti and high-Ti probably caused the differences in the relative abundances of plagioclase and pyroxene in these rocks. More Al_2O_3 may favour earlier plagioclase crystallization; more CaO may favour earlier Ca-rich clinopyroxene instead of feldspar. The overall result is the overlap in the CaO–MgO diagram at broadly the same MgO for both main groups.

Trace elements give indications on the relative abundance of the fractionating phases in the main groups: in the Sr–Zr diagram (Fig. 17) the high-Ti rocks show a clear positive trend, which can be interpreted as the result of clinopyroxene-dominated fractionation. This positive correlation is much weaker or absent in the low-Ti basalts, as a probable consequence of a major plagioclase-buffered evolution. It also noted that only some of the low-Ti basaltic andesites reach the Sr and Zr concentrations of the I-Ti basalts.

Major element mass balance calculations (Stormer & Nicholls, 1978) were carried out on selected samples, as far as possible from localities close together. The evolution from low-Ti picrites to evolved low-Ti basalts (D60–D146, SE Kathiawar), which gives the kink in the CaO–MgO diagram, was successfully modelled with a total of 38% fractionation of olivine (Fo_{81}), plagioclase (An_{74}) and augite ($Ca_{36}Mg_{52}Fe_{12}$) in the ratio 58:33:9 ($R^2 = 0{\cdot}19$). This result indicates that plagioclase and olivine played the most important role in the initial whole-rock trends, with the likely formation first of dunitic and then of allivalitic cumulates, and that clinopyroxene contribution is subordinate.

The transition from high-Ti picrite to basalt (D44–D128, central–western Kathiawar) was modelled by 54% fractionation of olivine, plagioclase, diopside and magnetite in the ratio 25:38:33:4 ($R^2 = 0{\cdot}15$). The clinopyroxene tends to be more important in the fractionation schemes for the early stages of differentiation.

The low-Ti basalt to low-Ti basaltic andesite transition (D208–D211, Rajpipla) was modelled by

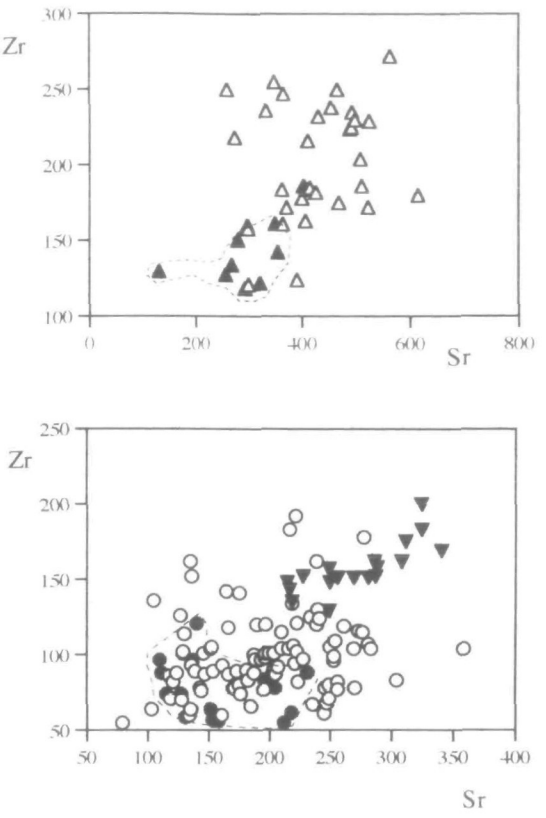

Fig. 17. Zr–Sr diagram for picrites, basalts and basaltic andesites of the various basalt groups. The normalized picrite values are also plotted. △, High-Ti; ▲, high-Ti picrites; ▼, I-Ti; ○, low-Ti; ●, low-Ti picrites.

~50% fractionation of olivine, plagioclase, augite and magnetite in the ratio 17:47:34:1 ($R^2 = 0{\cdot}33$), i.e. half of the crystal extract is made up of feldspar, and at this stage of evolution the subtracted assemblage is gabbroic. The contribution of clinopyroxene to the magmatic evolution is clearly larger at this fractionation stage. The transition from low-Ti basalt to 'andesite' (D45–D73, eastern Kathiawar) was modelled with 87% fractionation of olivine, plagioclase, augite and magnetite in the ratio 7:43:46:4 ($R^2 = 0{\cdot}15$). The very high crystal extract obtained in this transition probably explains the very low abundance of such differentiated rock types, as can be seen in the TAS diagram (Fig. 3a).

The mineral chemical variations from the basic to differentiated rocks, and from one group to another, strongly indicate different liquid lines of descent, i.e. the effects of significantly different physico-chemical conditions of crystallization. As an example, the different trends of the groundmass feldspars provide clear evidence for this. The lack of K enrichment in the late-crystallized feldspars of the low-Ti picrites to 'andesites', compared with the presence of anortho-

clase in the groundmass of some high-Ti picrites, indicates that, even at a differentiated stage of evolution, the rocks of a given group have common characteristics of crystallization.

The unusual stability of olivine as a microlitic phase in relatively differentiated, hypersthene-normative low-Ti rocks is also noteworthy. This feature can be justified only by the lack of a strong Si-enrichment trend, owing to *in situ* gabbro crystallization. This typically tholeiitic feature does not allow the incoming of a clear Si oversaturation into the groundmass, and, consequently, the presence of late Ca-poor pyroxenes. The latter are present, however, in some other low-Ti rocks. The prolonged stability of olivine may also suggest that extensive and uniform interaction with Si-rich crustal contaminants probably did not alter phase relationships. There is no evidence for the involvement of significant amounts of Fe–Ti oxides (and/or apatite) in the crystal fractionation sequence, at least down to basaltic andesites or 'andesites'. Finally, petrographic and geochemical evidence completely precludes any reasonable attempt to justify the negative Ti anomalies of the low-Ti rocks with simple crystal fractionation processes, at any degree of differentiation.

The presence of strongly differentiated dacites and rhyolites in the Gujarat area is interesting in the context of Deccan vulcanism. These rocks show some geochemical characters which may relate them to the spatially associated basalts, for instance the low Nb contents of the D16 rhyolite, found with low-Ti rocks, and the high Nb of the Pavagadh pitchstone (D89), found with high-Ti rocks. However, some other characters seem to exclude a direct genetic link, e.g. the high La/Nb ratio of the Pavagadh pitchstone, when compared with the relatively low La/Nb of all the high-Ti basalts. The possibility of significant crustal contamination processes, coupled with partial melting of intrusive equivalents of the spatially associated basalts, is probably an inescapable requirement, owing to the likely prolonged residence times of differentiated magmas in the crust. However, much more detailed geochemical and isotopic work is needed to confirm this hypothesis quantitatively.

DISCUSSION

The petrological and geochemical study of the Gujarat flood basalts has produced some features not evident in the central part of the Deccan Traps. In detail, it is recognized that a major part of the Kathiawar peninsula is covered by low-Ti, incompatible element-depleted basalts, with related differentiates. Further east, in the Rajpipla area, four magma groups (low-Ti, I-Ti, high-Ti and KT) are found interstratified. In the Kathiawar peninsula, south of a rough line connecting Rajkot to Palitana (Fig. 1b), no high-Ti or I-Ti rocks have been found; in contrast, the Pavagadh sequence is made up only of high-Ti rocks (and their spatially related high-REE–Nb rhyolites).

It is also noteworthy that rocks with geochemical characters identical to those of Kathiawar are still present to the south and east. In particular, we identified a group of lava flows in northwestern Maharashtra (Dhule area, south of the Tapti river and SE of Gujarat, Fig. 1a) which have low TiO_2 contents (1·2–1·5 wt %), as well as low Nb (<11 p.p.m.), Ti/V (20–24), Zr/Y (3·1–3·6) and MgO contents (5–7 wt %; L. Melluso, unpublished data, 1993). Another peculiarity of Gujarat is the presence of strongly enriched (and sometimes potassium-rich) basalts, relatively uncommon in the Kathiawar, but abundant in the Pavagadh and Rajpipla areas.

There is no evidence for a relatively uniform mantle source, as for the basic lavas of the Skye main lava series (Scarrow & Cox, 1995), or the flood basalts of West Greenland (Holm *et al.*, 1993). In some respects, the need for distinct mantle sources is similar that in the northern Lebombo–Nuanetsi area of the Karoo. The picrites of this area give evidence of two end-members, in particular an 'asthenospheric', Ca–Al-rich and incompatible trace element poor end-member (similar to a very depleted N-MORB) and a Ca–Al-poor and trace element rich (lamproitic) one (e.g. Cox *et al.*, 1984; Ellam & Cox, 1991; Fig. 14a). However, the low-Ti magmas of Lesotho, Nuanetsi and Malawi (and the very low-Ti Ferrar rocks in Antarctica) do not fit within the two end-members, as they need sources more Ti-depleted than N-MORB (Hergt *et al.*, 1989; Ellam & Cox, 1991).

There are some other significant differences also between the high-Ti picrites of Gujarat, the Nuanetsi–North Lebombo analogues (Cox *et al.*, 1984; Ellam & Cox, 1989) and the high-Ti basalts of the Paranà (Hawkesworth *et al.*, 1992), particularly in the absolute concentrations of many incompatible elements and in the striking negative Nb anomaly in the mantle-normalized diagrams of all Karoo and Paranà high-Ti (and low-Ti) basalts; this negative anomaly is completely absent in the high-Ti picrites, whereas is possibly present in the I-Ti basalts (Fig. 12).

As shown before, the major and HFSE contents of the low-Ti basalts of Gujarat show remarkable similarities to the rocks belonging to the Bushe Fm of the Western Ghats (Cox & Hawkesworth, 1985;

Lightfoot *et al.*, 1990; Fig. 12) and to the tholeiitic dykes of the Seychelles Islands (Devey & Stephens, 1991). Although these geochemical characters cannot be fruitfully used stratigraphically to correlate low-Ti and Bushe basalts (which may well be present at very different stratigraphic heights in the basalt sequence) it is suggested that the Bushe rocks, apart from the different genetic significance currently given to the LILE- and LREE-selective enrichment (shallow-level contamination by granitic melts; e.g. Mahoney, 1988) may have a common, HFSE-depleted mantle source region.

In contrast to the low-Ti rocks, the OIB-like nature of the high-Ti mantle-normalized patterns is demonstrated by a clear LREE enrichment, and relatively high concentrations of the other incompatible trace elements, particularly HFSE, even in the most basic rocks, and by the elemental ratios. This, in turn, implicates mantle sources distinct from those of the basalts of the Ambenali and Mahableshwar Fms (Fig. 12). Indeed, the trace element enrichment of the high-Ti picrites has no analogues in the Western Ghats lava pile (the basalts of the most enriched Mahableshwar Fm very seldom exceed 20 p.p.m. Nb; Cox & Hawkesworth, 1985; L. Melluso, unpublished data, 1993). Strongly enriched mantle sources were consequently present in northern Kathiawar and eastern Gujarat. The geochemistry of the high-Ti picrites seems to be significantly similar to that of the inferred parental magma of Reunion (Fisk *et al.*, 1988), the present-day expression of the probable hot-spot which generated the Deccan Traps. The Reunion data show, at identical MgO (15·4 wt %), slightly lower TiO_2 (1·7%) and Nb (23 p.p.m.) but generally similar incompatible element contents (Fig. 12), except for the most incompatible ones. This suggests that the high-Ti rocks of Gujarat may be considered as having been generated from substantially similar mantle sources, different from those of the Ambenali Fm. These latter basalts, at similar $^{87}Sr/^{86}Sr$ ($\sim$0·704; Lightfoot *et al.*, 1990) show different trace element contents and ratios from those of Reunion. In particular, the Ambenali basalts have very low K, Nb and K/Nb ratios (average 150; L. Melluso, unpublished data, 1993), which are different also from N-MORB values ($\sim$250; Sun & McDonough, 1989).

Relative to the high-Ti group the I-Ti basalts have distinct trace element enrichment patterns, and most probably have analogues in some of the chemical types of the lowermost formations of the Western Ghats (Jawhar, Igatpuri and Thakurvadi Fms; Beane *et al.*, 1986, 1988; Bodas *et al.*, 1988; Khadri *et al.*, 1988; Subbarao *et al.*, 1988; Sethna & Sethna, 1990; Peng *et al.*, 1994). Some relatively high La/Nb ratios (Table 7) and the relative depletion in Sr and P in the mantle-normalized diagrams (Fig.12) probably indicate a weak but significant crustal imprint for this group.

The data on the potassic rocks cropping out in the Rajpipla area are broadly similar to those of Krishnamurthy & Cox (1980) and Mahoney *et al.* (1985), albeit showing smaller compositional variations. These rocks show geochemical features more extreme than those of the high-Ti group, even considering their somewhat differentiated nature. The absence of negative K spikes in the KT mantle-normalized diagrams, which are usual in the high-Ti suite and in the Ambenali and Mahableshwar Fm rocks (Fig. 12), rules out different degrees of partial melting of similar sources, and suggests that the primary magmas of the group of potassic rocks could have been generated by differently enriched parts of the Deccan lithosphere, with the likely contribution of phlogopite (see Mahoney *et al.*, 1985). The sampling work in the Kathiawar peninsula, although it was not in great detail, failed to detect K-rich equivalents westwards; therefore, the metasomatized phlogopite-bearing mantle possibly did not extend farther west, and is to be considered only as a localized enrichment event in the Deccan Trap sources. The available data for the northern part of the western Ghats (e.g. Khadri *et al.*, 1988; Peng *et al.*, 1994) also confirm that potassic rocks are absent, and therefore they are probably confined to the Rajpipla area.

It is worth noting that, in recent times, some workers (Huppert & Sparks, 1985; Devey & Cox, 1987) proposed that an AEC process (assimilation coupled with equilibrium crystallization) could have been significant in the petrogenesis of some basalts of the Western Ghats; this process should have caused a positive correlation between compatible elements and some crustal-sensitive chemical parameters (LILE and $^{87}Sr/^{86}Sr$), as a consequence of crustal contamination acting on hotter and hotter Mg-rich rocks. No positive evidence for this is seen in the most basic rocks of Gujarat. Moreover, the correlation between MgO and LILE was observed in rocks of different formations, which have characters judged to derive from distinctly different mantle sources.

The estimates of pressure give some indications of the probable provenance of these magmas (from $\sim$90 km to $\sim$50 km). It is to be noted that an average lithospheric thickness of 110 km was calculated by Negi *et al.* (1986) for the Indian shield. This value is, however, variable also beneath the Deccan (from the present-day $\sim$50 km beneath Gujarat and Narmada–Tapti, close to or above post-Deccan

rifted areas, to ~120 km toward the south), and increases southwards to a value of ~180 km. The depth of the Moho in the Gujarat area (35–37 km; Gupta & Gaur, 1984) provides evidence that the most Si-rich picritic magmas equilibrated close to the Moho. A simple model that may be considered is that an adiabatically upwelling mantle, with a potential temperature of ~1430°C, began to melt slightly above the garnet stability field up to the Moho. However, the high inferred potential temperatures of the mantle beneath Gujarat give significant problems for the petrogenesis of the low-Ti picrites. Indeed, the strong decoupling of LILE from HFSE found in the low-Ti picrites is not a MORB (or plume) feature, and is usually found in rocks which interacted with continental material. Taking into account the high MgO contents of many of the low-Ti rocks of Gujarat and the absence of relationship between SiO_2 and LILE, it is argued that contamination during the ascent in the crust is not likely, and, consequently, that the relatively high LILE/HFSE ratios were inherited from a significant elemental contribution of the sub-Deccan lithosphere, which became heated and melted during mantle upwelling. The hypothesis of a significant lithospheric control for the petrogenesis of the low-Ti rocks of Gujarat may also be strengthened by the depleted major and trace element geochemistry, which implies stabilization in a relatively infertile mantle. This latter may be preferentially located beneath the Gujarat area, with respect to other parts of the Deccan, owing to the probable crustal displacement in the Narmada–Tapti region (Sen, 1991).

The origin from hydrous lithosphere hypothesized by Gallagher & Hawkesworth (1992) for many flood basalts cannot be confirmed by our data, as the Gujarat rocks seem to be almost completely devoid of hydrous minerals, and thus they should be considered as generated by very H_2O-undersaturated parent magmas (and, possibly, mantle sources).

As noted above, a clear correlation between the stratigraphy of Gujarat basalts and that of the Western Ghats is precluded by a gap in our knowledge south of the Narmada–Tapti sector and north of Igatpuri. Moreover, the lowermost recognized formations of the Western Ghats show very strong variability in their geochemical characters (Khadri *et al.*, 1988; Peng *et al.*, 1994), and the genetic significance of their trace element patterns (as well as those within a given formation) is still unclear.

CONCLUSIONS

The Gujarat Trap basalts comprise several petrographic and geochemical groups, apparently unrelated by fractional crystallization, and possibly generated from independent mantle sources:

(1) a low-Ti group, represented by picrite basalts to 'andesites', dominated in the early stages of differentiation by olivine (± chromite) and plagioclase fractionation. This group is characterized by some of the most depleted trace element contents so far reported in a CFB sequence, but with an evident decoupling of LILE from HFSE. This group is most widespread in the Kathiawar peninsula and shows some geochemical characters similar to rocks of the Bushe and Poladpur Fms of the central Deccan and to the Bushe-like tholeiitic dykes of the Seychelles Islands; there are no clear geochemical signs of crustal contamination in the picrites after their emplacement into the crust.

(2) A high-Ti group, with a similar compositional range (picrites to basaltic andesites and probably to rhyolites), but with a slightly more alkali-rich character, cropping out in the northern Gujarat and in the Rajpipla area; this group has much higher concentrations of strongly incompatible elements, and probably was generated by partial melting of fertile (i.e. cpx-rich) mantle sources; this group has strong affinities with OIB, and the trace element geochemistry of the high-Ti rocks is probably the best analogue of Reunion parental magmas up to now recorded in the Deccan Traps.

(3) An I-Ti group of basalts, characterized by distinctly lower incompatible element enrichment than for the high-Ti suite, which seems to have been generated from somewhat different mantle sources. It is perhaps similar to some chemical types of the lower formations of the Western Ghats (Jawhar to Thakurvadi);

(4) A potassium-rich group (KT), cropping out in the Rajpipla area, with a comparatively small compositional range, but extreme enrichment in K, Ba and Rb, which is tentatively related to locally significant amounts of phlogopite in its mantle source.

The differentiated rocks (dacites and rhyolites), although possessing some geochemical characteristics similar to those of the spatially associated basalts, are not strictly compatible with their derivation from basic magmas via simple crystal fractionation processes, and probably need at least some crustal contribution.

The distribution of these groups overlaps in the Rajpipla area, and in northern Kathiawar provides clear evidence for a strong spatial and vertical heterogeneity of the mantle beneath the western part of Deccan; moreover, the regional extent of the low-Ti basalts in the pre-drift position seems to suggest a

large and strongly HFSE-depleted mantle region, similar to most, if not all the other low-Ti sources elsewhere in the Gondwana CFB suites (see Hergt *et al.*, 1991).

It is evident that the mantle sources of this area of the Deccan were subjected to very complex histories, and that no simple mixing schemes between enriched and depleted sources can fit all the data. Moreover, there is no evidence for different P–T conditions of formation for low-Ti and high-Ti picrites.

Whatever may be the ultimate cause of the LILE-selective enrichment of the low-Ti rocks world-wide, this work provides clear evidence that: (1) the low-Ti rocks cannot be the crustally contaminated versions of high-Ti (or I-Ti) suites; (2) the mantle sources of low-Ti and high-Ti picrites are distinct also in their major element contents; (3) the mantle sources of low-Ti and high-Ti picrites suffered a completely different enrichment style.

There is evidence that low-Ti-related magma sources similar to those of Kathiawar did extend into parts of the Deccan, going farther south and west, and probably also that the Bushe basalts are geochemically associated with the low-Ti rocks of Gujarat.

Taking into account the rapid migration of the volcanic pile southwards, and supposing that the northernmost volcanics are stratigraphically older than the uppermost formations, namely Ambenali to Panhala [this is still strongly debatable, judging from the radiometric dates available up to now (see Baksi, 1994)], it is unreasonable to argue that the very strong heterogeneity of the Deccan mantle sources from north to south (evident regardless of any degree of contamination during the uprise in the crust) is related to differences within a rising plume without lithospheric contribution, particularly where the lithosphere is thick. This reinforces the conclusions of the authors that mantle lithosphere is at least a significant supplier to flood basalt volcanism (e.g. Erlank *et al.*, 1988; Ellam & Cox, 1991; Gallagher & Hawkesworth, 1992; Hooper & Hawkesworth, 1993; however, for asthenosphere-dominated models, see McKenzie & Bickle, 1988; Campbell & Griffiths, 1990; Arndt & Christensen, 1992). Further investigations on this topic cannot be made without detailed and comprehensive isotopic work on Gujarat basalts.

ACKNOWLEDGEMENTS

C. Garbarino (Cagliari), M. Serracino (Rome) and M. Coltorti (Ferrara) are gratefully thanked for their generous and skilled help in microprobe and X-ray fluorescence (XRF) analyses; S. F. Sethna (St. Xavier's College, Bombay) and K. V. Subbarao (Indian Institute of Technology, Bombay) have been very kind in providing hospitality, updated books and papers (and nice cups of tea) to L. Melluso; A. Canzanella (Napoli) patiently assisted in the daily setting of the XRF, and V. Monetti (Napoli) performed some key powder pellets. Comments of Colin Devey and Peter Hooper helped very much to improve an earlier version. The friendly and careful help and advice given by Keith Cox in the preparation of a revised manuscript is greatly appreciated, as are precious editorial comments of Brian Upton. This work was supported by MURST grants (40%).

REFERENCES

Albarède, F., 1992. How deep do common basaltic magmas form and differentiate? *Journal of Geophysical Research* **97,** 10997–11009.

Allan, J. F., Sack, R. O. & Batiza, R., 1988. Cr-rich spinels as petrogenetic indicators: MORB-type lavas from the Lamont seamount chain, eastern Pacific. *American Mineralogist* **73,** 741–753.

Andersen, D. J. & Lindsley, D. H., 1988. Internally consistent solution model for Fe–Mg–Mn–Ti oxides: Fe–Ti oxides. *American Mineralogist* **73,** 714–726.

Arndt, N. T. & Christensen, U., 1992. The role of lithospheric mantle in continental flood volcanism: thermal and geochemical constraints. *Journal of Geophysical Research* **97,** 10967–10981.

Backman, J., Duncan. R. A., *et al.*, 1988. Introduction. *Proceedings of Ocean Drilling Program, Initial Reports* 115. College Station, TX: Ocean Drilling Program, pp. 5–15.

Baksi, A. K., 1994. Geochronological studies on whole-rock basalts, Deccan Traps, India: evaluation of the timing of volcanism relative to the K–T boundary. *Earth and Planetary Science Letters* **121,** 43–56.

Baksi, A. K. & Farrar, E., 1991. $^{40}Ar/^{39}Ar$ dating of the Siberian Traps, USSR: evaluation of the ages of the two major extinction events relative to episodes of flood basalt volcanism in the USSR and the Deccan Traps, India. *Geology* **19,** 461–464.

Beane, J. E. & Hooper, P. R., 1988. A note on the picrite basalts of the Western Ghats, Deccan Traps, India. *Memoirs of the Geological Society of India* **10,** 117–133.

Beane, J. E., Hooper, P. R. & Subbarao, K. V., 1988. Petrogenesis of the Kalsubai and Lonavala subgroups, Deccan basalt group, India. In: *International Conference, Geochemical Evolution of the Continental Crust,* Poços de Caldas, Brazil, pp. 48–53.

Beane, J. E., Turner, C. A., Hooper, P. R., Subbarao, K. V. & Walsh, J. N., 1986. Stratigraphy, composition and form of the Deccan Basalts, Western Ghats, India. *Bulletin of Volcanology* **48,** 61–83.

Biswas, S. K., 1982. Rift basins in Western margin of India and their hydrocarbon prospects with special reference to Kutch basin. *Bulletin, American Association of Petroleum Geologists* **66,** 1497–1513.

Biswas, S. K., 1987. Regional tectonic framework, structure and evolution of the western marginal basins of India. *Tectonophysics* **135,** 307–327.

Bodas, M. S., Khadri, S. F. R. & Subbarao, K. V., 1988. Stratigraphy of the Jawhar and Igatpuri formations, Western

Ghat lava pile, India. *Memoirs of the Geological Society of India* **10**, 235–252.

Bose, M. K., 1973. Petrology and geochemistry of the igneous complex of Mount Girnar, Gujarat, India. *Contributions to Mineralogy and Petrology* **39**, 247–266.

Bowles, J. F. W., 1988. Definition and range of naturally occurring minerals with the pseudobrookite structure. *American Mineralogist* **73**, 1377–1383.

Boynton, W. V., 1984. Cosmochemistry of the rare earth elements: meteorite studies. In: Henderson, P. (ed.) *Rare Earth Element Geochemistry*. Amsterdam: Elsevier, pp. 63–114.

Brotzu, P., Capaldi, G., Civetta, L., Orsi, G., Gallo, G. & Melluso, L., 1992. Geochronology and geochemistry of Ferrar rocks from North Victoria Land, Antarctica. *European Journal of Mineralogy* **4**, 605–617.

Buddington, A. F. & Lindsley, D. H., 1964. Iron titanium oxide minerals and their synthetic equivalents. *Journal of Petrology* **5**, 310–357.

Campbell, I. H. & Griffiths, R. W., 1990. Implications of mantle plume structure for the evolution of flood basalts. *Earth and Planetary Science Letters* **99**, 79–93.

Carmichael, I. S. E., 1967. The iron titanium oxides of salic volcanic rocks and their associated ferromagnesian minerals. *Contributions to Mineralogy and Petrology* **14**, 36–54.

Cawthorn, R. G., de Wet, M., Hatton C. J. & Cassidy, K. F., 1991. Ti-rich chromite from the Mount Ayliff intrusion, Transkei: further evidence for high-Ti tholeiitic magma. *American Mineralogist* **76**, 561–573.

Courtillot, V., Besse, J., Vandamme, D., Montigny, R., Jaeger, J. J. & Cappetta, H., 1986. Deccan flood basalts at the Cretaceous/Tertiary boundary? *Earth and Planetary Science Letters* **80**, 361–374.

Cox, K. G. & Devey, C. W., 1987. Fractionation processes in Deccan Trap magmas: comments on the paper by G. Sen: Mineralogy and petrology of the Deccan Trap lava flows around Mahabaleshwar, India. *Journal of Petrology* **28**, 235–238.

Cox, K. G., Duncan, A. R., Bristow, J. W., Taylor, S. R. & Erlank, A. J., 1984. Petrogenesis of the basic rocks of the Lebombo. *Geological Society of South Africa, Special Publication* **13**, 149–169.

Cox, K. G. & Hawkesworth, C. J., 1984. Relative contribution of crust and mantle to flood basalt magmatism, Mahabaleshwar area, Deccan Traps. *Philosophical Transactions of the Royal Society of London, Series A* **310**, 627–641.

Cox, K. G. & Hawkesworth, C. J., 1985. Geochemical stratigraphy of the Deccan Traps at Mahabaleshwar, Western Ghats, India, with implication for open system processes. *Journal of Petrology* **26**, 355–387.

Devey, C. W. & Cox, K. G., 1987. Relationships between crustal contamination and crystallisation in continental flood basalt magmas with special reference to the Deccan Traps of Western India. *Earth and Planetary Science Letters* **84**, 59–68.

Devey, C. W. & Lightfoot, P. C., 1986. Volcanological and tectonic control of stratigraphy and structure in the western Deccan Traps. *Bulletin of Volcanology* **48**, 195–207.

Devey, C. W. & Stephens, W. E., 1991. Tholeiitic dykes in the Seychelles and the original spatial extent of the Deccan. *Journal of the Geological Society of London* **148**, 979–983.

Duncan, R. A. & Pyle, D. G., 1988. Rapid eruption of the Deccan flood basalts at the Cretaceous/Tertiary boundary. *Nature* **333**, 841–843.

Eggins, S. M., 1992. Petrogenesis of Hawaiian tholeiites: 1, phase equilibria constraints. *Contributions to Mineralogy and Petrology* **110**, 387–397.

Eggins, S. M., 1993. Origin and differentiation of picritic arc magmas, Ambae (Aoba), Vanuatu. *Contributions to Mineralogy and Petrology* **114**, 79–100.

Ellam, R. & Cox, K. G., 1989. A Proterozoic lithospheric source for Karoo magmatism: evidence from the Nuanetsi picrites. *Earth and Planetary Science Letters* **92**, 207–218.

Ellam, R. & Cox, K. G., 1991. An interpretation of Karoo picrite magmas in terms of interaction between asthenospheric magmas and the mantle lithosphere. *Earth and Planetary Science Letters* **105**, 330–342.

Erlank, A. J., Duncan, A. R., Marsh, J. S., Sweeney, R. J., Hawkesworth, C. J., Milner, S. C., Miller, R. McG. & Rogers, N. W., 1988. A laterally extensive geochemical discontinuity in the subcontinental Gondwana lithosphere. In: *International Conference, Geochemical Evolution of the Continental Crust*, Poços de Caldas, Brazil, pp. 1–10.

Fisk, M. R., Upton, B. G. J., Ford, C. E. & White, W. M., 1988. Geochemical and experimental study of the genesis of magmas of Reunion Island, Indian Ocean. *Journal of Geophysical Research* **93**, 4933–4950.

Franzini, M., Leoni, L. & Saitta, M., 1975. Revisione di una metodologia analitica per fluorescenza-X, basata sulla correzione completa degli effetti di matrice. *Rendiconti Società Italiana di Mineralogia e Petrologia* **31**, 365–378.

Frey, F. A., Green, D. H. & Roy, S. D., 1978. Integrated models of basalt petrogenesis: a study of quartz-tholeiites to olivine melilitites from south eastern Australia utilizing geochemical and experimental petrological data. *Journal of Petrology* **19**, 463–513.

Gallagher, K. & Hawkesworth, C. J., 1992. Dehydration melting and the generation of continental flood basalts. *Nature* **358**, 57–59.

Gallet, Y., Weeks, R., Vandamme, D. & Courtillot, V., 1989. Duration of Deccan trap volcanism: a statistical approach. *Earth and Planetary Science Letters* **93**, 273–282.

Glazner, A. F., 1984. Activities of plagioclase and olivine components and applications to geothermometry. *Contributions to Mineralogy and Petrology* **88**, 260–268.

Govindaraju, K. & Mevelle, G., 1987. Fully automated dissolution and separation methods for inductively coupled plasma atomic emission spectrometry rock analysis. Application to the determination of rare earth elements. *Journal of Analytical and Atomic Spectroscopy* **2**, 615–621.

Grove, T. L., Gerlach, D. C. & Sando, T. W., 1982. Origin of calcalkaline series lavas at Medicine Lake Volcano by fractionation, assimilation and mixing. *Contributions to Mineralogy and Petrology* **80**, 160–182.

Gupta, M. L. & Gaur, V. K., 1984. Surface heat flow and probable evolution of Deccan volcanism. *Tectonophysics* **105**, 309–318.

Gwalani, L. G., Rock, N. M. S., Chang, W.-J., Fernandez, S., Allegre, C. J. & Prinzhofer, A., 1992. Alkaline rocks and carbonatites of Amba Dongar and adjacent areas, Deccan igneous province, India: 1. Geology, petrography and petrochemistry. *Mineralogy and Petrology* **47**, 219–253.

Hawkesworth, C. J., Gallagher, K., Kelley, S., Mantovani, M. S. M., Peate, D. W., Regelous, M. & Rogers, N. W., 1992. Paraná magmatism and the opening of the South Atlantic. In: Storey, B. C., Alabaster, T. & Pankhurst, R. J. (eds) *Magmatism and the Causes of Continental Break-up. Special Publication, Geological Society of London* **68**, 221–240.

Hergt, J. M., Chappell, B. W., Faure, G., McCulloch, M. T., McDougall, I. & Chivas, A. R., 1989. Geochemical and isotopic constraints on the origin of the Jurassic dolerites of Tasmania. *Journal of Petrology* **30,** 841–883.

Hergt, J. M., Peate, D. W. & Hawkesworth, C. J., 1991. The petrogenesis of Mesozoic Gondwana low-Ti flood basalts. *Earth and Planetary Science Letters* **105,** 134–148.

Hirose, K. & Kushiro, I., 1993. Partial melting of dry peridotites at high pressures: determination of compositions of melts segregated from peridotite using aggregates of diamonds. *Earth and Planetary Science Letters* **114,** 477–489.

Hofmann, A. W., 1988. Chemical differentiation of the earth: the relationships between mantle, continental crust and oceanic crust. *Earth and Planetary Science Letters* **90,** 297–314.

Holm, P. M., Gill, R. C. O., Pedersen, A. K., Larsen, J. G., Hald, N., Nielsen, T. F. D. & Thirlwall, M. F., 1993. The tertiary picrites of West Greenland: contributions from 'Icelandic' and other sources. *Earth and Planetary Science Letters* **115,** 227–244.

Hooper, P. R., 1990. The timing of crustal extension and the eruption of continental flood basalts. *Nature* **345,** 246–249.

Hooper, P. R. & Hawkesworth, C. J., 1993. Isotopic and geochemical constraints on the origin and evolution of the Columbia River basalts. *Journal of Petrology* **34,** 1203–1246.

Huppert, H. E. & Sparks, R. S. J., 1985. Cooling and contamination of mafic and ultramafic magmas during ascent through continental crust. *Earth and Planetary Science Letters* **74,** 371–386.

Ishii, T., 1976. The relations between temperature and composition of pigeonite in some lavas and their application to geothermometry. *Mineralogical Journal* **8,** 48–57.

Jagoutz, E., Palme, H., Baddenhausen, H., Blum, K., Cendales, M., Dreibus, G., Spettel, B., Lorenz, V. & Wanke, H., 1979. The abundances of major, minor and trace elements in Earth's mantle as derived from primitive ultramafic nodules. *Proceedings of 10th Lunar Scientific Conference. Geochimica et Cosmochimica Acta Supplement,* 2031–2050.

Kaila, K. L., Tewari, H. C. & Sarma, P. L. N., 1981. Crustal structure from deep seismic sounding studies along Navibandar–Amreli profile in Saurashtra, India. *Memoirs of the Geological Society of India* **3,** 218–232.

Khadri, S. F. R., Subbarao, K. V., Hooper, P. R. & Walsh, J. N., 1988. Stratigraphy of Thakurvadi Formation, Western Deccan Basalt Province, India. *Memoirs of the Geological Society of India* **10,** 281–304.

Klein, E. M. & Langmuir, C. H., 1987. Global correlation of ocean ridge basalt chemistry with axial depth and crustal thickness. *Journal of Geophysical Research* **92,** 8089–8115.

Kostopoulos, D. K., 1991. Melting of the shallow upper mantle: a new perspective. *Journal of Petrology* **32,** 671–699.

Kostopoulos, D. K. & James, S. D., 1992. Parametrization of the melting regime of the shallow upper mantle and the effects of variable lithospheric stretching on the mantle modal stratification and trace element concentrations in magmas. *Journal of Petrology* **33,** 665–691.

Krishnamurthy, P. & Cox, K. G., 1977. Picrite basalts and related lavas from the Deccan Traps of Western India. *Contributions to Mineralogy and Petrology* **62,** 53–75.

Krishnamurthy, P. & Cox, K. G., 1980. A potassium-rich alkalic suite from the Deccan Traps, Rajpipla, India. *Contributions to Mineralogy and Petrology* **73,** 179–189.

Leake, B. E., 1978. Nomenclature of amphiboles. *Mineralogical Magazine* **42,** 533–563.

Le Bas, M. J., LeMaitre, R. W., Streckeisen, A. & Zanettin, P., 1986. A chemical classification of volcanic rocks based on the total alkali–silica diagram. *Journal of Petrology* **27,** 745–750.

Leoni, L. & Saitta, M., 1976. X-ray fluorescence analysis of 29 trace elements in rock and mineral standards. *Rendiconti Società Italiana di Mineralogia e Petrologia* **32,** 497–510.

le Roex, A. P., Dick, H. J. B., Reid, A. M., Frey, F. A., Erlank, A. J. & Hart, S. R., 1985. Petrology and geochemistry of the basalts from the American–Antarctic ridge, Southern Ocean: implications for the westward influence of the Bouvet mantle plume. *Contributions to Mineralogy and Petrology* **90,** 367–380.

Lightfoot, P. C. & Hawkesworth, C. J., 1988. Origin of Deccan Trap lavas: evidence from combined trace element and Sr-, Nd- and Pb-isotope data. *Earth and Planetary Science Letters* **91,** 89–104.

Lightfoot, P. C., Hawkesworth, C. J., Devey, C. W., Rogers, N. W. & Van Calsteren, P. W. C., 1990. Source and differentiation of Deccan Trap lavas: implications of geochemical and mineral chemical variations. *Journal of Petrology* **31,** 1165–1200.

Lindsley, D. H., 1983. Pyroxene thermometry. *American Mineralogist* **68,** 477–493.

Mahoney, J. J., 1988. Deccan Traps. In: Macdougall, J. D. (ed.) *Flood Basalts.* Dordrecht: Kluwer, pp. 151–194.

Mahoney, J. J., Macdougall, J. D., Lugmair, G. W., Gopalan, K. & Krishnamurthy, P., 1985. Origin of contemporaneous tholeiitic and K-rich alkalic lavas: a case study from the northern Deccan Plateau, India. *Earth and Planetary Science Letters* **72,** 39–53.

Mahoney, J. J., Macdougall, J. D., Lugmair, G. W., Murali, A. V., Sankar Das, D. & Gopalan, K., 1982. Origin of the Deccan Trap flows at Mahabaleshwar inferred from Nd and Sr isotopic and chemical evidence. *Earth and Planetary Science Letters* **60,** 47–60.

McDonough, W. F., 1991. Constraints on the composition of the continental lithospheric mantle. *Earth and Planetary Science Letters* **101,** 1–18.

McKenzie, D. P. & Bickle, M. J., 1988. The volume and composition of melt generated by extension of the lithosphere. *Journal of Petrology* **29,** 625–679.

Mellini, M., Carbonin, S., Dal Negro, A. & Piccirillo, E. M., 1988. Tholeiitic hypabyssal dykes: how many clinopyroxenes? *Lithos* **22,** 127–134.

Melluso, L., 1992. Caratteristiche petrologiche e geochimiche di vulcaniti continentali del Deccan, India. Ph.D. Thesis, Ferrara University.

Misra, K. S., 1981. The tectonic setting of Deccan volcanics in southern Saurashtra and Northern Gujarat. *Memoirs of the Geological Society of India* **3,** 81–86.

Mitchell, C. & Widdowson, M. 1991. A geological map of the southern Deccan Traps, India and its structural implications. *Journal of Geological Society of London* **148,** 495–505.

Najafi, S. J., Cox, K. G. & Sukheswala, R. N., 1981. Geology and geochemistry of the basalt flows (Deccan Traps) of the Mahad–Mahableshwar section, India. *Memoirs of the Geological Society of India* **3,** 300–315.

Negi, J. G., Pandey, O. P. & Agrawal, P. K., 1986. Super-mobility of hot Indian lithosphere. *Tectonophysics* **131,** 147–156.

Norrish, K. & Hutton, J. T., 1967. An accurate X-ray spectrographic method for the analysis of a wide range of geological samples. *Geochimica et Cosmochimica Acta* **33,** 431–453.

Papike, J. J., Cameron, K. E. & Baldwin, K., 1974. Amphiboles and pyroxenes: characterization of other than quadrilateral

components and estimates of ferric iron from microprobe data. *Geological Society of America, Abstracts with Programs* **6,** 1053–1054.

Paul, D. K., Potts, P. J., Rex, D. C. & Beckinsale, R. D., 1977. Geochemical and petrogenetic study of the Girnar igneous complex, Deccan volcanic province, India. *Geological Society of America Bulletin* **88,** 227–234.

Peng, Z. X., Mahoney, J. J., Hooper, P. R., Harris, C. & Beane, J. A., 1994. A role for continental crust in flood basalt genesis? Isotopic and incompatible element study of the lower six formations of the Western Deccan Traps. *Geochimica et Cosmochimica Acta* **58,** 267–288.

Ridley, W. I., 1977. The crystallisation trends of spinels in Tertiary basalts from Rhum and their petrogenetic significance. *Contributions to Mineralogy and Petrology* **64,** 243–255.

Roeder, P. L. & Emslie, R. F., 1970. Olivine–liquid equilibrium. *Contributions to Mineralogy and Petrology* **29,** 275–289.

Scarrow, J. H. & Cox, K. G., 1995. Basalts generated by decompressive adiabatic melting of a mantle plume: a case-study from the Isle of Skye, NW Scotland. *Journal of Petrology* **36,** 3–22.

Sen, G., 1986. Mineralogy and petrogenesis of the Deccan Trap lava flows around Mahabaleshwar. *Journal of Petrology* **27,** 627–663.

Sen, G., 1988. Possible depth of origin of primary Deccan tholeiite magma. *Memoirs of the Geological Society of India* **10,** 35–51.

Sen, N., 1991. The Narmada–Son–Brahmaputra transform: a Mesozoic fracture zone in Gondwanic India. *Tectonophysics* **186,** 359–364.

Sethna, S. F., 1988. Petrology and geochemistry of the acid, intermediate and alkaline rocks associated with the Deccan Basalts in Gujarat and Maharashtra. *Memoirs of the Geological Society of India* **15,** 47–61.

Sethna, S. F. & Sethna, B. F., 1988. Mineralogy and petrogenesis of Deccan Trap basalts from Mahabaleshwar, Igatpuri, Sagar and Nagpur areas, India. *Memoirs of the Geological Society of India* **10,** 69–90.

Sethna, S. F. & Sethna, B. F., 1990. Petrology of Deccan Trap basalt of the Western Ghats around Igatpuri and their petrogenetic significance. *Journal of the Geological Society of India* **35,** 631–643.

Stormer, J. C., Jr & Nicholls, J., 1978. XLFrac: a program for interactive testing of magmatic differentiation models. *Computers and Geosciences* **4,** 143–159.

Subbarao, K. V. (ed.), 1988. Deccan Flood Basalts. *Memoirs of the Geological Society of India* **10,** 393 pp.

Subbarao, K. V., Bodas, M. S., Hooper, P. R. & Walsh, J. N., 1988. Petrogenesis of Jawhar and Igatpuri Formations Western Deccan basalt province. *Memoirs of the Geological Society of India* **10,** 253–280.

Sun, S. S. & McDonough, W. F., 1989. Chemical and isotopic systematics of oceanic basalts: implications for mantle composition and processes. In: Saunders, A. D. & Norry, M. J. (eds) *Magmatism in the Ocean Basins, Geological Society Special Publication* **42,** 313–345.

Sweeney, R. J., Duncan, A. R. & Erlank, A. J., 1994. Geochemistry and petrogenesis of central Lebombo basalts of the Karoo igneous province. *Journal of Petrology* **35,** 95–125.

Sweeney, R. J., Falloon, T. J., Green, D. H. & Tatsumi, Y., 1991. The mantle origins of the Karoo picrites. *Earth and Planetary Science Letters* **107,** 256–271.

Tiwari, B. D., 1966. *The Geochemistry of the Volcanic Rocks of Pavagarh, Gujarat, India.* Banaras Hindu University Press, Varanasi, India, 156 pp.

Tiwari, B. D., 1972. Magmatic differentiation of the volcanics at Pavagarh, Gujarat, India. *Bulletin Volcanologique* **35,** 1129–1177.

Watts, A. B. & Cox, K. G., 1989. The Deccan Traps: an interpretation in terms of progressive lithospheric flexure in response to a migrating load. *Earth and Planetary Science Letters* **93,** 85–97.

West, W. D., 1958. The petrography and petrogenesis of forty-eight flows of Deccan Trap penetrated by borings in western India. *Transactions of the National Institute of Sciences of India* **4,** 1–56.

Wood, D. A., 1979. A variably veined sub-oceanic upper mantle—genetic significance for mid-ocean ridge basalts from geochemical evidence. *Geology* **7,** 499–503.

Yoder, H. S., Jr & Tilley, C. E., 1962. Origin of basaltic magmas: an experimental study of natural and synthetic rock systems. *Journal of Petrology* **3,** 342–532.

RECEIVED JANUARY 5, 1994
REVISED TYPESCRIPT ACCEPTED APRIL 3, 1995

APPENDIX: ANALYTICAL TECHNIQUES

Whole-rock major element analyses have been performed at Ferrara, Milano and Perugia universities, utilizing pressed powder pellets and fused glass discs, according to the methods of Franzini *et al.* (1975) and Norrish & Hutton (1967). Loss on ignition (LOI), Na_2O and MgO have been analysed with standard gravimetric and atomic absorption spectroscopy (AAS) methods, respectively. Trace elements Sc, V, Cr, Ni, Cu, Zn, Rb, Sr, Y, Zr, Nb, Ba and Th have been analysed at Napoli and Ferrara, with two PW1400 XRF spectrometers, utilizing pressed powder pellets, Rh and W anodes at Napoli, W at Ferrara, and following the data reduction method of Leoni & Saitta (1976). Detection limits are in the p.p.m. order for most low-level trace elements; precision is within ± 1 p.p.m. at the 0–10 p.p.m. range, and better than 10% for the other ranges; to avoid bias, some key trace element analyses (mostly in the rocks with $>10\%$ MgO) have been performed with a single XRF (Napoli). REE have been analysed at CRPG, Nancy, France, following the methods described by Govindaraju & Mevelle (1987). Microprobe analyses have been performed at Cagliari University, utilizing silicates and oxides as standards, an ARL-SEMQ instrument and the MAGIC IV correction method; a subset of the analyses has been performed at CNR-CSGIC, Rome, utilizing a CAMECA SX-50 and the PAP correction method. Bias between the two microprobes has been found to be negligible.